



Faculty of technology

Evaluation of a snowmobile track motion resistances with multibody dynamics simulation

Ari Pesonen

Mechanical Engineering

Master's thesis

June 2022

ABSTRACT

Evaluation of a snowmobile track motion resistances with multibody dynamics simulation

Ari Pesonen

University of Oulu, Degree Programme of Mechanical Engineering

Master's thesis 2022, 74 pp. + 3 Appendixes

Supervisor(s) at the university: Tuutijärvi Miro–Tommi

In this work, target is to build and validate a simulation model of a snowmobile track entity with multibody dynamics simulation software Adams. A full vehicle snowmobile simulation model is also explored. Before there has been a problem with the track model being inaccurate. The focus on this thesis is on implementing a track model, but a full vehicle model is also discussed and presented as the work with the model will continue. Existing tracked vehicle theory is studied and presented how Adams tracked vehicle plugin utilizes these theories.

Research consists of simulations with the track model were driven with a real snowmobile and measured for torque and velocity data. Model validation proves that the track model acts quite accurately up to 25 km/h drive speed but with 50 km/h speed the model becomes unstable. With 10 km/h speed simulation result error is 19,87 % and with 25 km/h simulation result error is 1,17 %. In the future the model will be further improved with building a proper chassis and validating the full vehicle model. Knowledge gained from this thesis may be used with simulating a snowmobile before production phase accurately and the model can be used for studying the motion resistances of a snowmobile track. This type of track model may be built to any tracked vehicle and validated in the way done in this thesis.

Keywords: Tracked vehicle, Snowmobile, Multibody–dynamics, Adams, Motion resistances

TIIVISTELMÄ

Moottorikelkan telaston ajovastuksien määrittäminen monikappaledynamiikka
simuloinnilla

Ari Pesonen

Oulun yliopisto, Konetekniikan tutkinto-ohjelma

Diplomityö 2022, 74 s. + 3 liitettä

Työn ohjaaja(t) yliopistolla: Tuutijärvi Miro–Tommi

Tässä työssä tavoitteena on rakentaa ja validoida moottorikelkan telaston simulointimalli Adams ohjelmistolla. Telastomallin lisäksi tarkastellaan myös kokonaisen moottorikelkan simulointimallia. Aiemmin on ollut ongelmana telamattomallin epätarkkuus. Työssä keskitytään etenkin kumitelamattomallin implementointiin, mutta kokonaista ajoneuvokokoonpanoa arvioidaan lisäksi, sillä työ mallin kanssa jatkuu. Olemassa olevaa tela-ajoneuvoteoriaa tutkitaan ja esitetään, kuinka Adamsin tela-ajoneuvo lisäosassa hyödynnetään kyseisiä teorioita.

Tutkimus koostuu simulaatioista telamattomallilla sellaisilla nopeuksilla, joita tutkimuksen aikana on mitattu todellisesta moottorikelkasta vääntötiedon kanssa. Validoinnissa todistetaan, että telamalli käyttäytyy suhteellisen tarkasti 25 km/h nopeuteen asti, mutta 50 km/h nopeudessa malli muuttuu epävakaaaksi. 10 km/h nopeudella simulaatiotuloksien virhe on 19,87 % verrattuna mitattuihin tuloksiin ja 25 km/h nopeudella simulaatiotuloksien virhe on 1,17 % verrattuna mitattuihin tuloksiin. Tulevaisuudessa mallia tullaan kehittämään lisäämällä siihen runkomalli ja validoimalla täydellinen ajoneuvokokoonpano. Työstä saatavaa tietoa voidaan hyödyntää tulevaisuuden moottorikelkkasimulaatioissa tarkan tiedon saavuttamiseksi ja nykyisellään mallia voidaan hyödyntää telastosta johtuvien ajovastusten tutkimiseen. Työssä esitellyn mallin rakennustavan pohjalta voitaisiin rakentaa telasto mihin tahansa tela-ajoneuvoon ja validoida se työtä vastaavalla tavalla.

Avainsanat: Tela-ajoneuvo, Moottorikelkka, Monikappaledynamiikka, Adams, Ajovastukset

ALKUSANAT

Tämä työ on tehty osana yritykseen tehtävää projektitutkimusta marraskuun 2021 ja kesäkuun 2022 välillä. Kesän 2021 aikana mietin diplomityön tekemistä ja suuntaa mihin haluaisin lähteä työurallani etenemään aiemmalta kunnossapitopainotteiselta polultani. Diplomityöaihe ajautui yllättäen eteeni ja kun ajattelin asiaa, aihe vaikutti erittäin mielenkiintoiselta. Aihe oli myös erittäin haastava ja työn edistyminen olikin erittäin palkitsevaa, sillä simulointikokemusta minulla ei ollut käytännössä lainkaan monikappaledynamiikan osalta.

Haluan kiittää Oulun yliopiston henkilökunnasta etenkin työni ohjaajaa Miro–Tommi Tuutijärveä ja Perttu Niskasta sekä muita projektiryhmäläisiä. Työt jatkuvat, mutta välissä nautitaan kesästä.

Kiitos Joonas Mähöselle korvaamattomasta avusta simulointiin liittyvissä kysymyksissä. Kaltaisesi huippuammattilaisen kanssa on ollut ilo ja kunnia työskennellä. Kiitos myös Petri Makkoselle simulointiavusta.

Oulussa 16.6.2022

Ari Pesonen

TABLE OF CONTENTS

ABSTRACT

TIIVISTELMÄ

ALKUSANAT

TABLE OF CONTENT

MARKINGS AND ABBREVIATIONS

1 Background	8
2 Multibody dynamics	9
2.1 Software	9
2.2 Adams	9
2.3 Theory	10
2.4 Adams solver.....	11
2.4.1 GSTIFF	12
2.4.2 WSTIFF	12
2.4.3 HASTIFF	12
2.4.4 HHT	12
2.4.5 Newmark.....	12
2.4.6 Index options	13
2.4.7 Corrector options	13
2.5 Solving procedure	13
3 Tracked vehicle theory.....	16
3.1 Tractive performance of a tracked vehicle	17
3.1.1 Normal pressure on terrain	18
3.1.2 Shear stress	22
3.1.3 Motion resistances	25
3.1.4 Tractive effort	26
3.1.5 Drawbar pull	26
3.2 Terzaghi's bearing capacity theory	26
4 Laboratory measurements	30
4.1 Track properties	30
4.2 Friction	36
5 ADAMS modelling and theory	37
5.1 Snowmobile structure.....	37
5.2 Modelling procedure	38
5.3 Rear suspension entity.....	40

5.4 Track	42
5.5 Timoshenko beam model	45
5.6 Drivetrain sprocket.....	45
5.7 Impact function	48
5.8 Contact function	49
5.9 Motor.....	50
5.10 Front suspension.....	53
5.11 Chassis.....	55
5.12 Adams Car hard road	55
5.13 ATV soft soil.....	57
6 Simulations.....	60
7 Results.....	62
7.1 Type 1 10 km/h	63
7.2 Type 1 25 km/h	64
7.3 Type 1 50 km/h	65
7.4 Type 2 20 km/h	65
7.5 Evaluation of the results.....	67
7.5.1 Type 1 10 and 25 km/h evaluation	67
7.5.2 Type 1 50 km/h evaluation	67
7.5.3 Type 2 20 km/h evaluation	67
8 Conclusions.....	69
9 Summary	70
References	72
ATTACHMENTS:	
Attachment 1. Tractive performance calculations	
Attachment 2. Adams model definitions	
Attachment 3. MATLAB code for result analysis	

MARKINGS AND ABBREVIATIONS

A	area of the track (segment)
b	the lesser dimension of penetrating contact/the contact width of the track/total width of the track segment
b_b	the contact width of the belly
C	cohesion of the soil (table value)
c	the damping coefficient of soil (table value)
c_{\max}	the maximum damping coefficient
d	the penetration value when maximum damping coefficient is applied
e	exponent of the force deformation characteristic
F	tractive effort of the vehicle
F_a	The aerodynamic drag force
F_m	force of mass carried by the track
F_q	the equilibrium equation in the direction of generalized coordinate q
$F_{\mu s}$	ski resistance force
h	the depth of grouser in soil
h_b	the grouser depth (soil depth z)
I	the slip of the track
K	shear deformation parameter
K_c	a pressure sinkage parameter for a soil (table value)
K_r	the fraction of the shear at which the curve falls off towards
K_{ω}	the shear displacement j on shear stress peak
K_{φ}	the tangent of the internal friction angle for a soil (table value)
k	the stiffness of the surface interaction
L	the Lagrangian ($T - V$) where T = kinetic energy and V = potential energy
l	the distance between point P and start point of shearing/reshearing
l_b	the contact length of the belly
l_g	the grouser length
l_s	the length limit
l_t	the contact length of the track
$m_{\#}$	# of constraint equations ($< \text{ or } = n$)
n	a pressure sinkage parameter for a soil (table value)
$n_{\#}$	# of generalized coordinates

p_0	normal pressure developed by the track
p_b	the normal pressure developed by the belly
R_G	the snowmobile gear ratio
Q	generalized force
q	generalized coordinate
r	the radius of the drive sprocket
T_A	the measured torque
T_R	the torque running the sprocket
t	time
V	vehicle velocity
V_j	slip velocity
V_t	theoretical velocity of the vehicle
V_z	the vertical velocity
W	the vertical load on the track segment
X	X – axis
x	the horizontal x axle distance between point P and start point of shearing/reshearing
x_p	the expression of a distance variable ie. displacement between two markers
z	the penetration depth
α	the angle between tangent of a track point P and the horizontal
α_b	the angle between belly and terrain horizontal
η	the efficiency of the transmission
τ	Shear stress
τ_b	the shear stress of the belly
ω	the angular velocity of the drive sprocket
λ	Lagrange multiplier
Φ	angle of internal shearing resistance of the terrain (table value)
Φ_a	algebraic constraint equation
\dot{x}	the derivative of x
x_1	specifies free length of x

1 BACKGROUND

Understanding about a snowmobile track motion resistances is important for minimizing the energy consumption of the vehicle. In future snowmobiles, it is important to minimize energy consumption because of sustainable development. In future vehicles, energy consumption minimization is important for green values and longer drive range. Optimizing energy consumption might lead to competition advantages that cannot be obtained without deep understanding about the motion resistances of a snowmobile. In this thesis is discussed how to evaluate snowmobile track motion resistances using MSC ADAMS multibody simulation software. Objective is to build a simulation model with a track implemented and the model to be modular for easy modifications. Existing tracked vehicle theory is presented and discussed how Adams implements it, multibody dynamics is discussed, simulation models of a snowmobile rear suspension–track entity and a full snowmobile model are presented, and the models are validated with data acquired from a real snowmobile. Possible limitations to the model accuracy and usage are incorrect or lacking parameters required by Adams.

2 MULTIBODY DYNAMICS

Multibody dynamics is widely referred to MBD abbreviation. MBD simulation aims to solve interactions between rigid or flexible parts in a system that may consist of two or more parts and how that system affects its environment. MBD analysis is based on MBS (multibody system). An MBS consists of mechanical components with the degrees of freedom and kinematic joints that limit the motions of the degrees of freedom. (Flores 2015, p. 1-2)

2.1 Software

On the market there are several commercial MBD software such as Adams by MSC-software, Simpack by Dassault Systems and Recurdyn by Functionbay. Software developers market especially Recurdyn and Adams to be well suited for different vehicle simulations. (MSC 2022 a; Functionbay 2022)

Free and open access based MBD programs are usually limited outside of commercial usage. Free and open access programs don't usually have user support, or support is possibly delayed. As an example, mbdyn is developed by Politecnico di Milano and FreeDyn is an Austrian based program. Free programs are good option instead of commercial software for academic purposes and if user finds suitable software for their application, but they lack advanced features that are built in commercial software to be used in simulations as with vehicles. In practice this means more user work hours as many commercial software automated features need to be done by hand. An example for this is the track wrapping feature on Adams tracked vehicle (ATV) package or EDEM Altair markets as a tool for accurate soil behaviour simulation with off-road vehicles. (MBDYN 2022; Freedyn 2022; Altair 2022)

2.2 Adams

Adams is commercial MBD software developed by MSC software. Adams consists of the base program that can be used for basic MBD simulations and with add-ons it can be enhanced to be more easily used for different applications. Adams Car-add-on makes it possible to build and simulate different vehicles more easily than with the basic software. Adams Car-add-on can be further enhanced with ATV-plugin that makes possible to

build and simulate tracked vehicles on soft drive terrain. In this thesis ATV–plugin is utilized to build a snowmobile rear suspension entity and simulate a complete snowmobile assembly with the built rear suspension.

2.3 Theory

When comparing MBD simulation with finite element analysis (FEA) simulation it can be said that both types of analyses aim to solve system change after its being affected by loads but put simply FEA is the best suited for the very small transformations of points in a part of system, while MBD is suited for very big transformations of fewer points between parts of a system. MBD solves non-linear problems with a few points the best while FEA solves a problem with more points to define the more exact distribution of stresses or shape of deformation (McConville 2015, p. 15). Therefore, MBD solving is used for defining motions between the pieces rather than motion of a piece.

In practice an MBS uses so called generalized coordinates to define the positions of the mechanical component. These generalized coordinates are defined in the “hardpoints” of Adams (discussed in 5.2) (Flores 2015, p. 12). In short, a generalized coordinate is a point defining a part where the degrees of freedom have effect with kinematic joints.

3D–MBD models have typically 6 degrees of freedom that are 3 translational motion axes and 3 rotational motions around these three axes defining the motion of a part in a system. The kinematic joints may limit movements for 1 or more degrees of freedom. The mechanical parts that have the degrees of freedom are often rigid but with more sophisticated models, flexible parts may be used. If the part is rigid, it won’t change shape unlike flexible part under forces. Flexibility adds more degrees of freedoms to the part (Flores 2015, p. 1) and therefore the model becomes more demanding to solve for a computer. Adding flexibility is not recommended if there is no obvious need for it.

MBD analysis on Adams is based on Lagrangian dynamics. The system equations of motion are constructed numerically and solved as the functions of time as presented in function 1 and 2 according to McConville (McConville 2015, p. 9):

$$F_j = \frac{d}{dt} \left(\frac{\partial L}{\partial \dot{q}_j} \right) - \frac{\partial L}{\partial q_j} + \sum_{i=1}^{m\#} \frac{\partial \phi_q^T}{\partial q_j} \lambda_i - Q_j = 0 \quad \text{for } j=1, \dots, n\# \quad (1)$$

$$\phi_i = 0 \quad (2)$$

Where:

- q is generalized coordinate,
- F_j is the equilibrium equation in the direction of generalized coordinate q,
- L is the Lagrangian (T - V) where T = kinetic energy and V = potential energy,
- Φ_a is algebraic constraint equation,
- λ is Lagrange multiplier,
- Q is generalized force,
- $n_{\#}$ is # of generalized coordinates,
- $m_{\#}$ is # of constraint equations (< or = n).

Known methods for building the MBS equations, besides the Lagrangian method are the Baumgarte method, the Penalty method and the Augmented Lagrangian method. The Baumgarte method modifies the Lagrangian method in order to make the solutions more stable, but in other hand increasing the risk of incorrect solution if incorrect constants are used (Flores 2015 p. 63–64).

The penalty method builds the equations of motion completely different to the Lagrangian and the Baumgarte method with 2nd order differential equation and it makes possible to solve problems with redundant constraints or kinematically singular configurations.

The Augmented Lagrangian method differentiates from the standard Lagrangian method with its solving of the equations of motion by an iterative process. (Flores 2015, p. 66)

2.4 Adams solver

Adams version 2021.2.2 that is utilized in this thesis has 5 different dynamic problem integrator solver options. They are GSTIFF, WSTIFF, HHT, Newmark and Hastiff. These solvers use implicit time integration. Unlike GSTIFF, WSTIFF and Hastiff, HHT and Newmark don't use backwards differentiation formula (BDF) that is explained as an example of solving procedure in Chapter 3.5. As a general notion some versions of Adams have explicit solver option, but it is very rarely used. Choosing a solver that fits the best problem in hand is very important for maximizing the usage of computational resources,

keeping the solution robust and having accurate solutions. (McConville 2015 p. 120–121; MSC 2021 c)

2.4.1 GSTIFF

GSTIFF is the default solver in Adams that has practically a solving procedure as described in Chapter 3.5. Solutions with GSTIFF may fail with very short time step in certain conditions. It also may also produce anomalies in results with predicting polynomial order greater than 2 and solver index setting being I3. These anomalies are seen in results as the short duration spikes of acceleration and speed when the displacement between time steps is zero. (McConville 2015, p. 120; MSC 2021 c)

2.4.2 WSTIFF

Generally, WSTIFF solver is a slower solver than GSTIFF. This is because the algorithm used avoids anomalies that GSTIFF solver has with predicting polynomials. In practice this results in more complex computations. Other than that solving procedure is the same as it is with GSTIFF. (McConville 2021, p. 120; MSC 2021 c)

2.4.3 HASTIFF

Hastiff solver uses predicting polynomials the way WSTIFF does and it allows SI1 index usage. (McConville 2021, p. 121)

2.4.4 HHT

HHT solver's way of operation can be described as a low pass filter cutting higher frequency spurious oscillations away. It updates Jacobian at every solution step and has predicting polynomial up to 2nd order. One problem with using this solver is that it overdamps solutions often but if dampening is not an issue with the problem it is a suitable solver to use. According to McConville: "it is finding increased usage in Adams". (McConville 2015, p. 121; MSC 2021 c)

2.4.5 Newmark

This solver is rarely used probably due to predictor limitation to order 1. Other than that, it works the way HHT does. (McConville 2015, p. 121; MSC 2021 c)

2.4.6 Index options

Choosing the index option for the solver is very important as it effects the computational time significantly. It also effects the stability of the simulation. Generally, I3 is faster, but less stable option, SI2 is slower than I3 but more stable and SI1 even slower but more stable than SI2. All these index options are not available on all the integrators. (McConville 2015, p. 121; MSC 2021 c)

2.4.7 Corrector options

These options are used to further enhance solver solution time and possibly solve error situations. User can change step size, permitted error tolerance, add interpolation as a step forwarding method instead of step time size control etc. Settings available depend on the chosen solver. (McConville, 2015, p.121–122; MSC 2021 c)

2.5 Solving procedure

Solving procedure of a step in Adams can be explained as in Figure 1 in accordance with McConville when using BDF solver. It is so called Adams predictor–corrector method. Other known solving procedures are Euler method and Runge–Kutta method (Flores 2015, p. 68). The most important difference between these solving methods is that Adams predictor- corrector algorithm utilizes the knowledge from the previous time step, unlike Runge–Kutta and Euler methods and because of this the solution should be faster to compute as the time step and function order are selected more appropriately in the beginning and therefore the computer needs to do less work for the solution. With Runge–Kutta and Euler methods the solver is “stupid” it does every step from the beginning, and it must do more calculations because of this. (Flores 2015, p. 72)

Though Adams predictor corrector method is advanced as it uses former time step solutions to predict the next step, it still needs starting values calculated with some other method as it is not self-starting (Flores 2015, p. 73). Flores says: “In short, the Adams methods, when being carefully used, are more efficient than any other method” (Flores 2015, p. 73). This phrase will be correct with any advanced MBD software solver that uses some type of predictive algorithms, not only Adams.

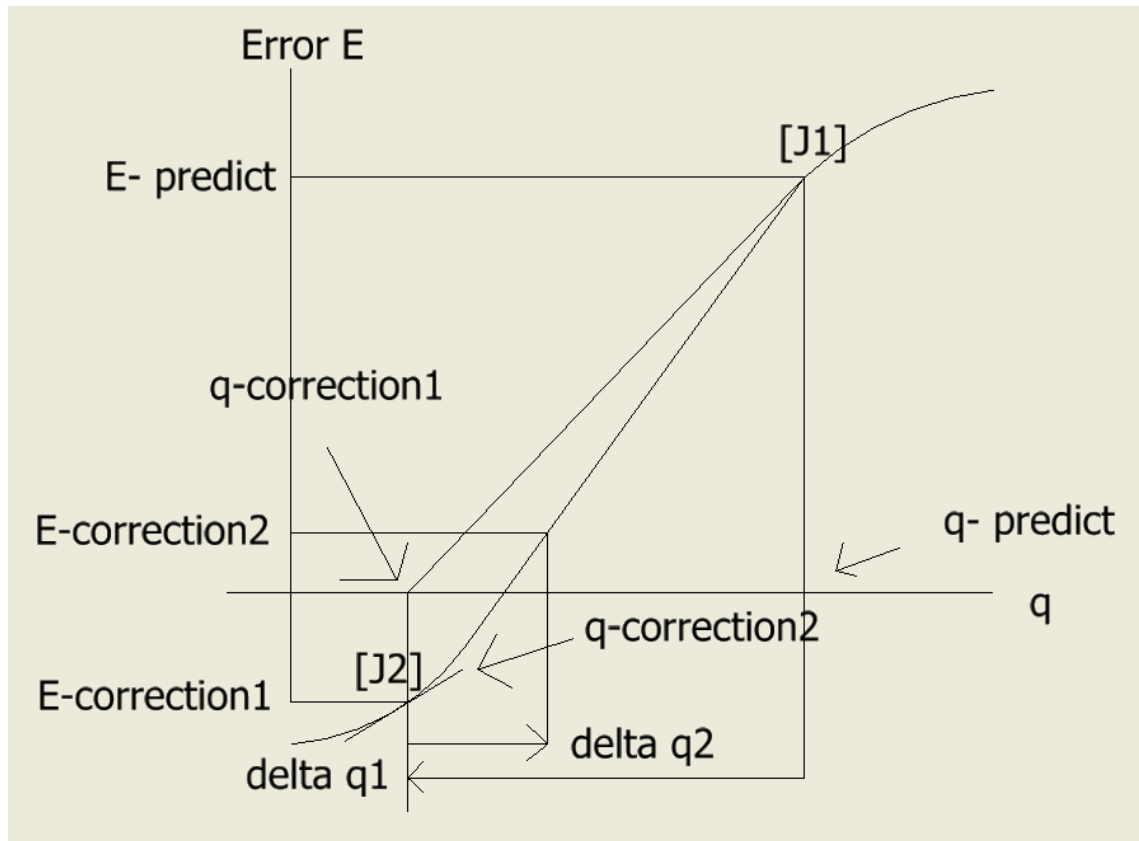


Figure 1. Newton-Raphson iteration retell as McConville presents (McConville 2015, p. 12).

As presented in Figure 1, at First with Newton Raphson iteration procedure q is predicted and when equilibrium is not met the result is error E as seen in the Figure. If the error is more than what the solver was defined acceptable by the user, solver will not proceed time forward but starts numerically differentiating q around the first predicted q . This way error change with changing of q will be determined and it is possible to determine Jacobian (J) that is the tangent of n -dimensional error hyper plane, in this example $n=1$. If error criteria set by the user can't be met, modifications to the predicted q are done with Newton-Raphson iteration according to functions (3) and (4):

$$E + \left[\frac{\partial E}{\partial q} \right] \Delta q = E + [J] \Delta q = 0 \quad (3)$$

$$\Delta q = -[J]^{-1} E \quad (4)$$

After modifications to q if the error criteria are not achieved, solver reduces time step and repeats the process described above. This can be done several times until solver reaches satisfying solution if plausible. The integrator will discard the step and return to

previously converged time step if the corrected q converges but the change in q does not satisfy remainder limit of the Taylor series expression of the predicting polynomial. Solver then tries a new step with a less aggressive predictor time step and the whole procedure explained above is done again until solver reaches simulation time or simulation step amount it was defined to reach. (McConville 2015, p. 11–13)

3 TRACKED VEHICLE THEORY

Publications and studies focusing on tracked vehicle multibody dynamics or a track of tracked vehicle are typically about steel track and military vehicle applications. Existing studies about a track are limited to farming and construction vehicle applications or to slower running speeds than a snowmobile typically runs. Mocera and Nicolini built a simple tracked farming vehicle Adams model with a track (2017), but it is built to run with 5 km/h max speed, so this type of simple model is not suitable for a snowmobile as the non-linear behaviour of rubber material will affect the model depending on the velocity a track is run. Mocera et. al (2020) further improved the track model with adding deformable terrain – track interaction to the farm vehicle Adams model.

Allen (2006) presents how non-linearity of rubber material affects a tracked vehicle track damping and stiffness values, but the study is made for a steel track with rubber bushings, not a full track.

Campanelli et al. (1998) present a method for dynamic stress and vibration evaluation of steel track links and conclude that reaction and contact forces are the most significant considering dynamic stresses on a track link.

Chołodowski and Dudziński (2019) tested track belt bending moment concluding that increasing track thickness, speed and tension increases the bending moment of a track. They also conclude that decreasing radius of a track bending shape increases bending moment needed to bend the track. Chołodowski et al. (2021) improve knowledge of internal energy consumption of a track evaluating energy losses developed by the vibrations of the track. They present methods to calculate the bending stiffness and internal damping of the track and conclude that in theory losses caused by vibrations are small in comparison to the losses developed by the wheels bending the track unless high amplitude vibrations with the low linear velocity of the track are present. Effect of dampening to vibration is small according to the study.

These studies by Chołodowski et al. confirm that MBD analysis with Adams will be well suitable for evaluation of a snowmobile track motion resistances even if there are minor inaccuracies with the damping values of the model as the most important values are the track running speed, the bending radiuses, the tension of the track and the thickness of

the track. Vibrations are not as important for result accuracy. (Chołodowski and Dudziński 2019; Chołodowski et al. 2021)

Tracked vehicle movement theory is explained in J.Y.Wongs book "Theory of ground vehicles". Wong bases his studies mostly on Bekker's studies that are presented in his book "Theory of land locomotion". Wongs studies are also presented in his book "terramechanics and offroad vehicle engineering" with a more practical approach as in the book is presented several empirical methods in order to define performance for an off-road vehicle. Understanding about terramechanics is needed to understand the vehicle–terrain interactions. ATV–plugin bases its theoretical background to the books of Wong and Bekker according to the ATV–plugin developer Slättenger. (Slättenger 2000)

3.1 Tractive performance of a tracked vehicle

When considering a tracked vehicle mobility one of the most important knowledge areas is the tractive performance of the vehicle. When tractive performance is defined accurately, it is possible to evaluate vehicle mobility in different conditions. Wong presents two methods in order to calculate tractive performance of a tracked vehicle as a function of the track slip. The first method was first presented by Bekker and Wong refined this model with his own model. Bekker's method has a more simplistic approach to the track–terrain interaction evaluation and therefore in this work is also discussed a more sophisticated Wongs method that takes in pressure and shear differentiation along the track–terrain interface. (Wong 2008 p. 147 and p. 149)

After the normal pressure and the shear stress distributions are defined it is possible to calculate track motion resistance, the tractive effort of the track and the drawbar pull force of the vehicle. Considering a snowmobile as a full vehicle, motion resistances developed by the skis and air drag force must be added to the total motion resistance. When a tracked vehicle belly is in contact with terrain, as in the case of the snowmobile running on deep snow, there is also belly drag caused by friction of the snow–belly contact. (Wong 2008, p. 149 and p. 162–163)

In attachment 1 is presented an example calculation of a snowmobile tractive performance calculations in Excel table based on the tracked vehicle theory presented in chapter 3.

3.1.1 Normal pressure on terrain

As discussed earlier, terrain under a snowmobile is under stress by the track, skis and in some situations the skid plate (called hull in Adams and belly in the literature). This causes normal pressure to be applied on the terrain and it deforms the terrain. Considering a snowmobile running on soft soil such as snow, the force equilibrium of the snowmobile can be presented as in Figure 2.

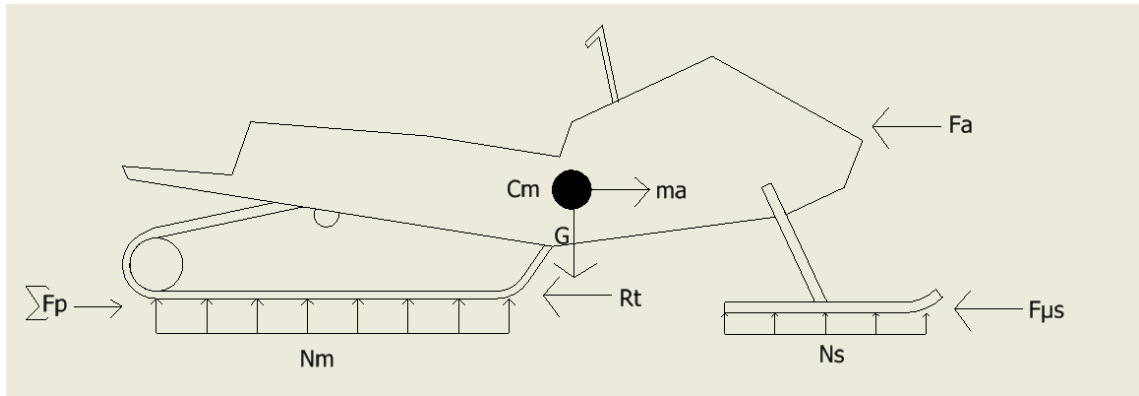


Figure 2. Snowmobile with forces acting on it.

Soil is put under vertical pressure by the track and skis. As presented in Figure 2, N_m (track supporting force) and N_s (ski supporting force) present forces that support the vehicle on the snow. F_a is the aerodynamic drag force, $m a$ is the force accelerating or decelerating the vehicle, $F_{\mu s}$ is the ski friction force, R_t is the track resistance force and ΣF_p is the summary of the tractive forces developed by the grousers. Shape of the supporting forces can be trapezoidal and have spikes depending on the position of the centre of mass of the vehicle and terrain obscurities. The skid plate or “belly” of a snowmobile may also add vertical pressure force to the terrain if the snowmobile is driven on soft enough soil such as deep snow. (Wong 2008, p. 162).

On soft or deep snow deformation may be visually significant, and it can be examined from a rail left behind by the snowmobile. If driving on hard enough terrain, this deformation is insignificant and the track lies flat on the terrain so there is no need to take deformation of the terrain into account at any calculations (Wong 2008, p. 158).

According to Wong a situation where a generic tracked vehicle, i.e., a tank, is deforming terrain can be described as in Figure 3 where track wheels passing a point of terrain cause a repetitive cycle of the pressure increase and decrease. The track is idealized to function

as a flexible belt and the pressure on the terrain increases and decreases according to the shape of the track and the repetitive loading cycle graphs of terrain (Wong 2008, p. 158–159). Shape of the track is limited by the track wheels (Wong calls them road wheels) and in the case of a snowmobile the track rails.

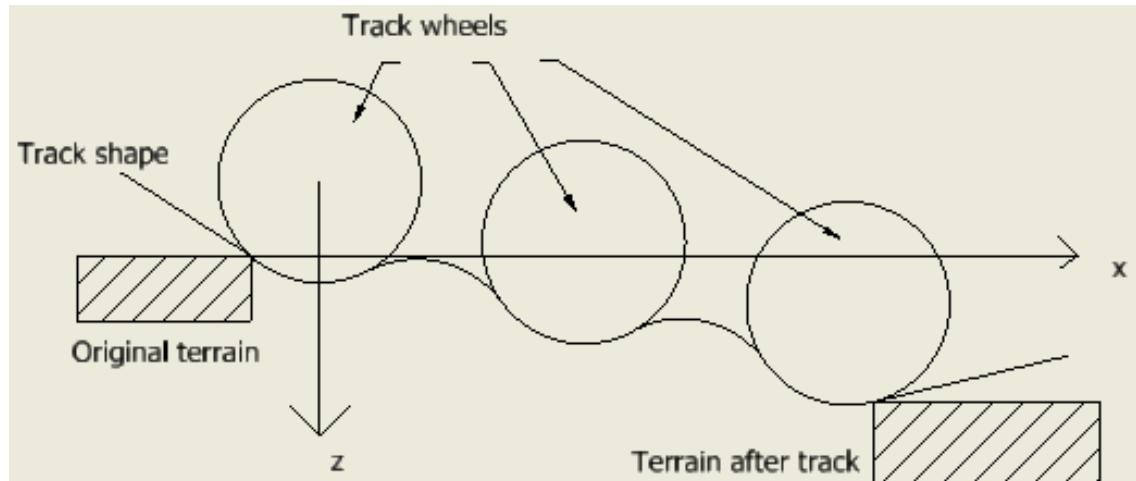


Figure 3. Track reshaping terrain retell as Wong presents (Wong 2008, p. 159).

As presented in Figure 3, the pressure on terrain increases when the tangent of the shape line of the track is going towards negative z -direction and decreases when the tangent is going towards positive z -direction. As the terrain point won't return to the height that it was before any deformation, the repetitive nature of the cycle causes always the next track wheel to deform the terrain more towards negative z -direction. Because of this the more rear of the track system is examined, the deeper it runs in the terrain. This causes the vehicle to run “nose up” (Wong 2008, p. 160). This behaviour might be useful in situations where the vehicle is close to get stuck, so it tries to “crawl” out of the situation, but in other hand it increases the motion resistance as some vehicle tractive effort is not used on forward motion.

The amount of pressure as a function of sinkage while a tracked vehicle is running over terrain area is described by the repetitive loading cycle graphs (Wong 2008, p. 137). A difficulty in using repetitive loading cycle graphs in snow terrain is that there is not just one type of snow. Snow is somewhat different everywhere. Snow acts differently depending on several parameters such as humidity and temperature. In Finland, this can be observed during different times of the day in winter or even the different phase of winter (comparing snow in January vs snow in April). When working with snow as terrain, it should be considered making measurements determining exact snow

parameters, if possible, to get the most accurate data for the simulation model. Slättenger says:” The experience has clearly shown that it is extremely hard to get successful simulations out from guessed data. The better the data is, the better the simulations will run” (Slättenger 2000). The data accuracy is very important when working with Adams ATV as inaccurate data will make solutions very often not to converge or the simulation will not be stable. In this thesis snow measurements are not done but existing table data values are used because of the time-consuming measurements needed for snow parameters to be defined.

When considering a snowmobile, the pressure increase–decrease cycle is simple to describe as the track rail keeps the pressure somewhat constant from the whole length of the track by the width from track rail left outer wall to track rail right outer wall. Therefore, Bekker’s simplified method of calculating the tractive effort of a snowmobile is suitable for a snowmobile calculation. The track shape can’t change more towards positive z -direction than what the rail describes. This behaviour is presented in Figure 4 below. Figure 5 presents a track rail of a snowmobile for reference.

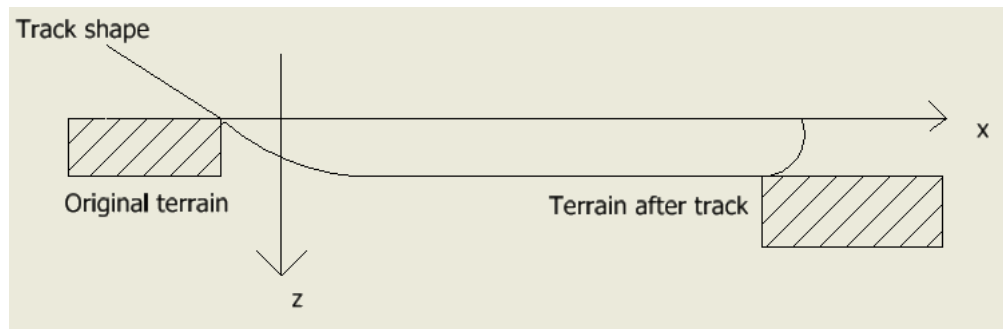


Figure 4. Terrain reshaping under a snowmobile track side view.

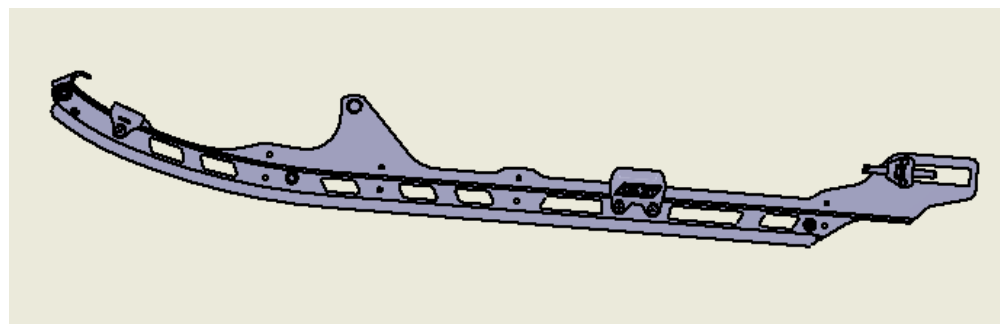


Figure 5. Track rail of a snowmobile.

The supporting track wheels on a snowmobile do not act exactly as the wheels on some generic tracked vehicle described by Wong. The supporting wheels support the track making it more rigid and possibly removing unwanted bending motions, but they can be removed, and the track system would still work because of the track rail would be supporting the track. However, in Figure 6 is shown how the track would bend when driven on soft terrain. The pressure developed by the track to the soil would be as Wong 2008, p. 91 presents. The supporting wheels and track rails would penetrate soil more and the bending centre part of the track would penetrate less of the soil. This affects the pressure developed by the track by decreasing it towards the middle of the track.

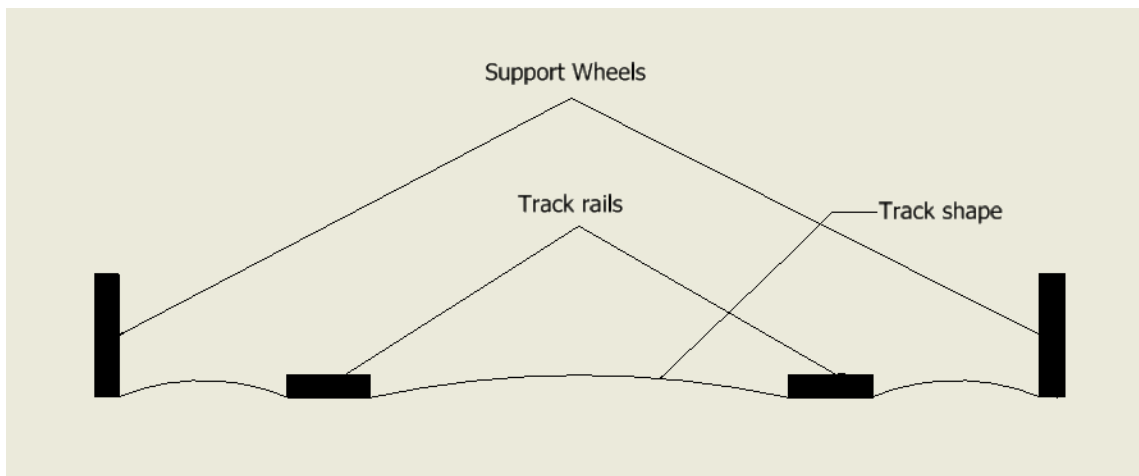


Figure 6. Track shape rear view.

If the track rails were to be removed and the track would be supported only by the supporting wheels, the situation would be close to as in Figure 4 described when looking from either side of the track system, but from rear view (Figure 6) the track shape curve would have just 1 radius.

According to Wong and Bekker normal pressure p_0 developed under a track of a tracked vehicle can be determined as an idealized uniform strip load (Wong 2008, p. 91–92). As discussed before, the track of the snowmobile is supported by the track rail. For viscous damping to have effect on the vertical load vertical speed and damping coefficient must be also known. Adams adds damping to the equation to make numerical calculations more stable with the simulation. With this knowledge p_0 right under a track is determined with function (5) (Wong 2008, p. 91; MSC 2015 e, s8–8):

$$p_0 = \frac{Fm}{A} + c * V_z \quad (5)$$

Where: p_0 is normal pressure developed by the track,
 F_m is force of mass carried by the track,
 A is area of the track (segment),
 c is the damping coefficient of soil (table value),
 V_z is the vertical velocity.

The uniform strip load develops stress on the soil. The soil may be idealized as an ideal elastoplastic material. The stress on the soil is maximized in the middle of a track decreasing linearly to 0 by function of depth and angle of 45 degrees from both sides of the track. (Wong 2008, p. 91)

If p_0 and soil parameters are known soil penetration is possible to solve from function (6) as Bekker presents (Wong 2008, p. 127; MSC 2015e, s8–5):

$$p_o = (K_c / b + K_\phi) z^n \quad (6)$$

Where: z is the penetration depth,
 b is the lesser dimension of penetrating contact,
 K_ϕ is the tangent of the internal friction angle for a soil (table value),
 K_c is a pressure sinkage parameter for a soil (table value),
 n is a pressure sinkage parameter for a soil (table value).

The soil parameters are defined with using a tool called bevameter (Wong 2008, p. 126) for exact parameters on certain soil type. In this thesis soil parameters are not of more interest as they demand time-consuming field measurements with the bevameter tool. Existing soil parameter table values are used with calculations and simulations. (Wong 2008, p. 130)

3.1.2 Shear stress

Shear stress distribution and magnitude are needed to calculate vehicle forces that make the vehicle move forward. To calculate shear stress distribution under a track first must be determined the magnitude of the track slip. Slip velocity is the difference of the velocity the track is running and the vehicle velocity at a point of time. The slip happens when the vehicle distributes enough driving force to overpass the friction developed by the track or when the terrain under the track deforms caused by the shear stress developed

by the track. The shear stress–soil displacement curve with dry fresh snow acts close to the ideal elastoplastic material stress–strain curve. Practically this means that with soft terrain the shear stress first increases linearly until the soil starts to deform with constant value. This behaviour is theoretical but comparing field measurement curves to theoretical curves has proven that the behaviour is close to the ideal elastoplastic material. (Wong p.138 and 140, MSC 2015 e s8–9)

According to Wong the slip speed of the tracked vehicle is determined with function (7) (Wong 2008, p.160):

$$V_j = V_t - V \cos \alpha = r\omega[1 - (1 - i) \cos \alpha] \quad (7)$$

Where: V_j is slip velocity,
 V_t is theoretical velocity of the vehicle,
 V is vehicle velocity,
 α is the angle between tangent of a track point P and the horizontal x axis,
 r is the radius of the drive sprocket,
 ω is the angular velocity of the drive sprocket,
 i is the slip of the track.

With the slip determined it is possible to calculate the shear displacement j . The shear displacement is used to define shear stress caused to the terrain. The easiest way to define V_j is with the tracked vehicle running straight and measuring the speed of the vehicle and comparing that with a GPS speed signal.

Shear displacement j is calculated with function (8) (Wong 2008, p. 161):

$$\begin{aligned} j &= \int_0^t r\omega[1 - (1 - i) \cos \alpha] dt \\ &= \int_0^l r\omega[1 - (1 - i) \cos \alpha] \frac{dl}{r\omega} \\ &= l - (1 - i)x_p \end{aligned} \quad (8)$$

Where: l is the distance between point P and start point of shearing/reshearing,
 x_p is the horizontal x axle distance between point P and start point of shearing/reshearing,
 t is time.

Maximum shear stress (τ_{max}) a soil withstands before starting to deform with constant value is determined as a function of normal pressure soil is under. Cohesion and the angle of internal shearing resistance of the terrain are to be determined with the bevameter soil test. Existing table data may be used. τ_{max} is defined with function (9) (Wong 2008, p. 97; MSC 2015, s8–11):

$$\tau_{max} = C + p_0 * \tan \phi \quad (9)$$

Where: Φ is angle of internal shearing resistance of the terrain (table value),
C is cohesion of the soil (table value).

With shear displacement and the stress defined it is possible to present shear stress displacement graph as Janosi and Hanamoto and Mohr–Coulomb failure criterion propose with function (10) (Wong 2008, p. 141; MSC 2015e, s8–11):

$$\tau = (C + p_0 \tan \phi)(1 - e^{-j/K}) \quad (10)$$

Where: K is a shear deformation parameter defining the shear stress displacement needed to develop the maximum shear stress.

K can be defined in two ways. Looking at a shear stress– displacement curve defined by the function 5 (Figure 7), K may be determined from the slope between zero and maximum of τ or from one third of displacement at 95% of maximum of τ . In practice K is defined with bevameter soil tests.

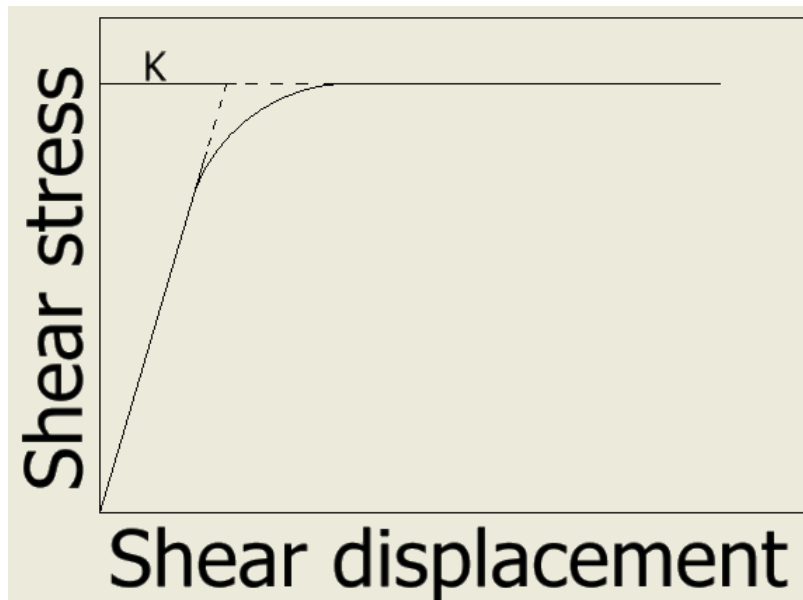


Figure 7. Shear stress – displacement dependency retell as Wong presents (Wong 2008, p. 140).

3.1.3 Motion resistances

With normal stress distribution and shear stress distribution known the motion resistances of a tracked vehicle can be calculated. The track has external motion resistance and when driving terrain that is very deformable the vehicle belly may take contact with the terrain. This is very likely to happen for example when snowmobile is driving on soft snow. On this event happening it causes some pressure from the track to be reduced and added to the vehicle “belly”. This causes drag force known as belly drag (Wong, p. 162–163). Also, there is the motion resistance of the skis that is function of N_s and the resistance coefficient between the ski and the terrain. When considering the whole vehicle and its motion resistances it is of interest to focus on the minimization of these forces as well.

The external motion resistance of the track is calculated with accordance to Wong with function (11) (Wong 2008, p. 163):

$$R_t = b \int_0^{l_t} p_0 \sin \alpha \, dl \quad (11)$$

Where: b is the contact width of the track,
 l_t is the contact length of the track.

If the belly (the skid plate of a snowmobile) of the vehicle is in contact with the ground, belly drag is determined with function (12) (Wong 2008, p. 163):

$$R_{be} = b_b \left[\int_0^{l_b} p_b \sin \alpha_b dl + \int_0^{l_b} \tau_b \cos \alpha_b dl \right] \quad (12)$$

Where: b_b is the contact width of the belly,
 l_b is the contact length of the belly,
 α_b is the angle between belly and terrain horizontal,
 p_b is the normal pressure developed by the belly,
 τ_b is the shear stress of the belly.

3.1.4 Tractive effort

A snowmobile has 1 track. Therefore, tractive effort F of a snowmobile track is calculated in accordance with Wong with function (13) (Wong 2008, p. 163):

$$F = b \int_0^{l_t} \tau \cos \alpha dl \quad (13)$$

Where: F is the tractive effort of the vehicle.

3.1.5 Drawbar pull

Drawbar pull is the force that is available for the tracked vehicle for towing after external motion resistance and belly drag are reduced from the tractive effort of the vehicle. Drawbar pull is determined with function (14) (Wong 2008, p. 164):

$$F_d = F - R_t - R_{be} \quad (14)$$

Where: F_d is the drawbar pull force.

3.2 Terzaghi's bearing capacity theory

The method described in chapter 3.1 is suitable for defining the tractive effort of a vehicle that already exists and is possible to measure as it demands the track slip defined with measured speed. It is obviously possible to calculate a tractive effort chart for a tracked vehicle with 0–100 % slips and therefore compare the results afterwards with the measured data. Adams ATV utilizes Terzaghi's bearing capacity theory (MSC 2020 d) to calculate the track– terrain interaction forces of a tracked vehicle.

Terzaghi's bearing capacity theory describes the force that affects a grouser when its penetrating terrain's surface. The force is used for evaluating the tractive performance developed by the grousers of a track. Terzaghi's theorem unites pressure developed into the soil by function 1 and the soil pressure by depth effect on calculating the force acting on the grouser surface. Function (15) presents the passive earth pressure according to Terzaghi's theory (MSC 2015 e; MSC 2020 d; Wong 2008, p. 104):

$$\sigma_p = \gamma_s z N_\phi + q N_\phi + 2c * \sqrt{N_\phi} \quad (15)$$

Where: γ_s is the specific weight of the soil,
 N_ϕ is the flow value of the soil = $\tan^2(45^\circ + \phi/2)$,
 q is the share of the total pressure p_0 developed by the segment i.e., 25 grousers are developing thrust $\rightarrow q$ is approximately 1/25 of p_0 .

With passive earth pressure defined force affecting a grouser of a track segment is defined with function (16) according to the Terzaghi's theory. Tractive force F_p is defined on every grouser in contact with the ground separately (MSC 2015 e; MSC 2020 d; Wong 2008, p. 105):

$$F_p = \int_0^{h_b} \sigma_p dz \quad (16)$$

Where: h_b is the grouser depth (soil penetration depth z).

The total tractive effort of a track is the summary of F_p values on every track segment.

Functions (15) and (16) are suitable for defining the tractive performance in a situation bulldozing effect is affecting the soil. Bulldozing happens when the distance between the grousers of the track is so large that the soil deforms between the grousers. Bulldozing is defined to happen when function (17) result is bigger than the distance between the grousers (MSC 2020 d):

$$l_s = \frac{h_b}{\tan\left(45^\circ - \frac{\phi}{2}\right)} \quad (17)$$

Where: l_s is the length limit.

If l_s is smaller than the distance between the grousers, the bulldozing effect will not happen, but the soil between grouser tips moves with the track (Figure 8):

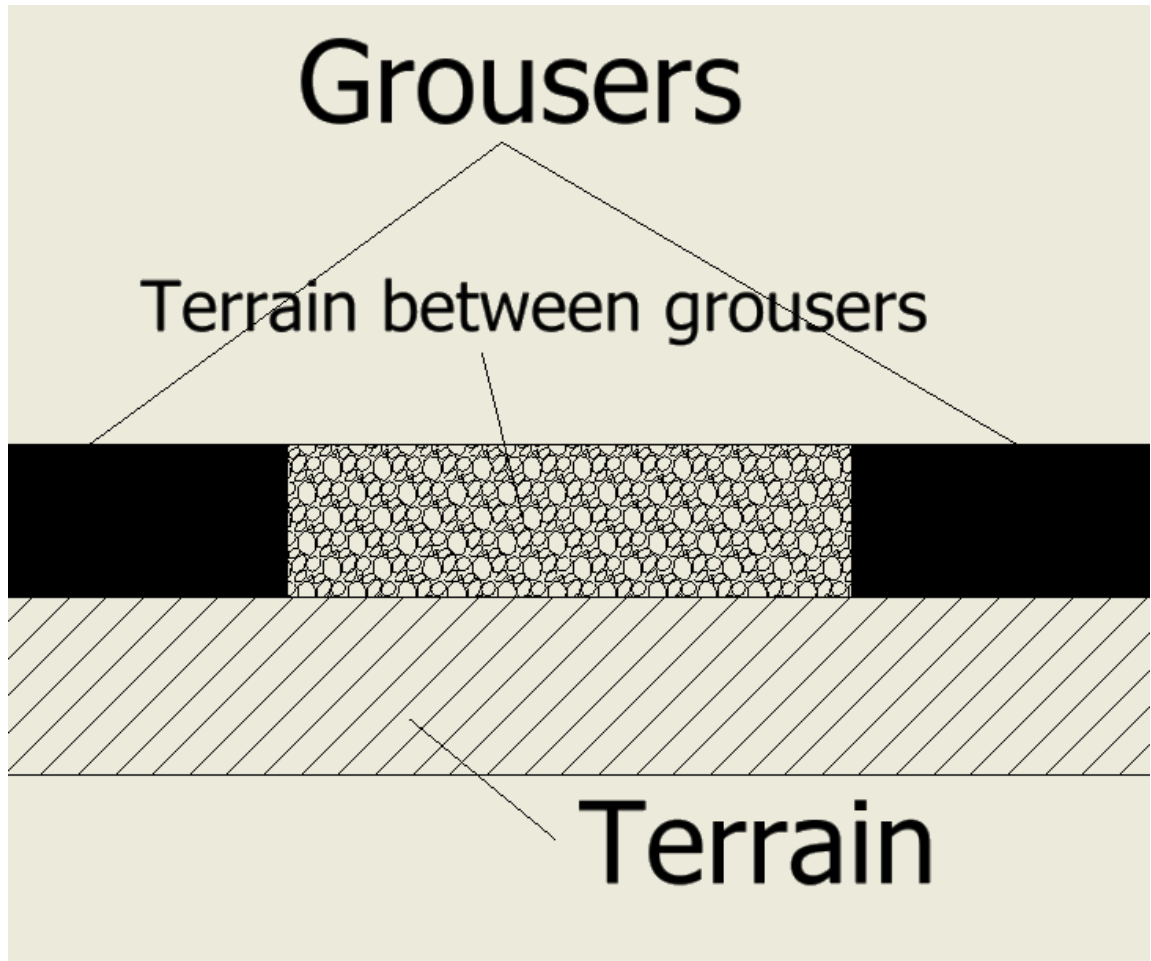


Figure 8. soil moving between grousers retell as ATV documentation presents (MSC 2020 d).

When bulldozing does not affect the soil, the total tractive force of a track segment is defined with function (18) (MSC 2020 d):

$$F_{\text{long}} = A_{\text{shoe}}(\tau_{\text{ext}} * gr + \tau_{\text{int}}(1 - gr)) \quad (18)$$

Where:

- A_{shoe} is the area of the grouser tip,
- τ_{ext} is the shear stress between grouser tip and the soil,
- τ_{int} is the shear stress between the moving soil and the undisturbed soil,
- gr is the ratio of the grouser tip area and the track segment area.

Grouser side walls add some traction. The side wall force added to the tractive force is calculated with function (19) (MSC 2020 d):

$$H_{side} = 2l_g hc + W \tan \phi \left(0.64 \frac{h}{b} \cot^{-1} \left(\frac{h}{b} \right) \right) \quad (19)$$

Where: l_g is the grouser length,
 h is the depth of grouser in soil,
 b is total width of the track segment,
 W is the vertical load on the track segment.

As p_0 is defined to be a uniform strip load W depends on the amount of track segments.
Therefore, $W = p_0 / \text{amount of track segments}$.

4 LABORATORY MEASUREMENTS

Laboratory measurements are necessary part of MBD simulation model validation. As discussed before, without correct parameters it is impossible to gain accurate results. It is necessary to define rubber track properties and frictions within the snowmobile rear suspension entity.

4.1 Track properties

Adams models a track with track segments that are linked to each other with segment connections (further discussed in chapters 5.4 and 5.5). For the proper behaviour of the track, it is necessary to define stiffness and damping values of a track segment joints with measurements. The parameters are very important to achieve robust, accurate and stable simulations with Adams ATV.

Adams segment connection definition example is shown in Figures 9, 10 and 11. The parameters to be defined are translational stiffnesses and damping (axes x, y and z), rotational stiffness and dampening (around axes x, y and z) and non-linearity (translational longitudinal stiffness parameters K1–5). Frequency scaling allows the material model to behave according to the frequencies it is vibrating. Frequency scaling is defined as a 1st degree polynomial spline. The frequency scaling (Figure 12) allows the model to scale the stiffness/damping values according to driving speed. It is defined by the different Hz values and according stiffnesses.

Crossterm values are not necessary as the model is simplified to bend from only the segment connection.

Modify a Track Segment

Track Segment Name:

Reference Frame:

Geometry Setting: ☒ Standard ☐ User Geometry

Include 2D Geometry: ☐ Yes ☒ No

Track Type: ☐ Steel Track ☒ Rubber Track

Track Configuration: ☐ Single ☒ Double

Track Pitch:

Connector Length:

Pin Radius:

Mass Properties | **Geometry** | **Segment Connection**

Connection Force

Unload Angle:

Translation Stiffness:

Translational Damping:

Rotational Stiffness:

Rotational Damping:

Crossterm Stiffness:

Crossterm Damping:

Field Longitudinal Stiffness: ☐ Standard ☐ Linear ☒ Nonlinear

Nonlinear Stiffness Values:

Frequency Scale Enabled: ☒ Yes ☐ No

Frequency Property File:

Field Attachment Offset: ☒ Yes ☐ No

Segment Field Attach. Offset:

Connector Field Attach. Offset:

Force Graphics:

OK Apply Cancel

Figure 9. Random track segment definitions.

The track segment is defined mass properties (mass and inertia values), the geometry of a parametrized track segment, and segment connection variables.

The track segment connection is defined non-linear stiffness behaviour with K-values. Deformation-force curve is automatically presented in the track segment non-linear stiffness editor.

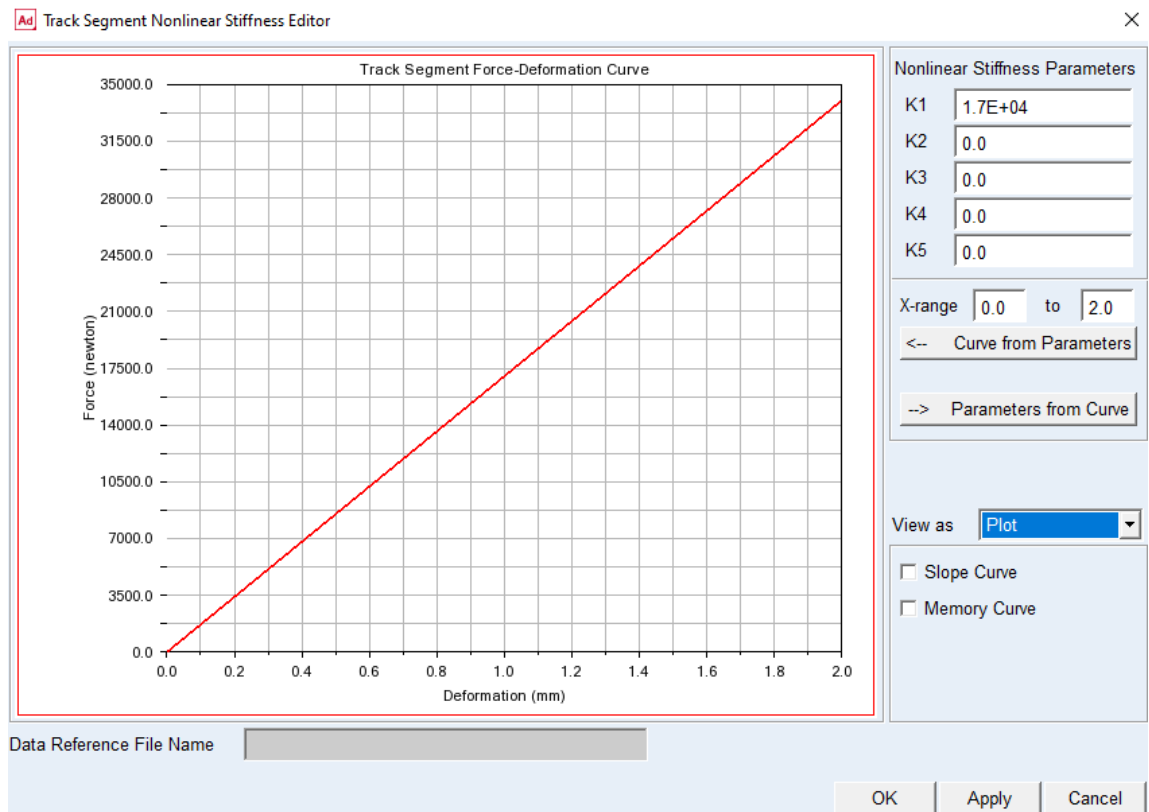


Figure 10. Track segment nonlinear stiffness editor.

The figure shows the 'ATV Curve Manager' window. It has a menu bar (File, Edit, View, Settings, Help) and a toolbar with a track segment icon and navigation arrows. Below the toolbar are fields for 'Starting Row' (1) and 'Number of Rows' (1), with 'Insert Rows' and 'Delete Rows' buttons. A 'Filter' field contains 'XX.XXX' and a 'Sort' button. The main area is a table with two columns: 'Velocity (mm/second)' and 'Scale (-)'. The table contains six rows of data.

	Velocity (mm/second)	Scale (-)
1	0.0	1.0
2	20.0	1.01
3	40.0	1.02
4	60.0	1.04
5	80.0	1.07
6	100.0	1.11

Figure 11. Frequency scaling editor.

Frequency scaling is added with velocity dependency with the Frequency scaling editor.

The track parameters used in this thesis are provided by Metropolia University of Applied Sciences as they have the equipment needed for making necessary measurements to a

track. Metropolia uses an MTS 100 Cyclic measurement device that allows static and dynamic applying of forces to a material piece multi axially. The device applies linear and torsional forces, so it is possible to define translational and rotational stiffnesses and dampening that are required by Adams.

The measurements done by Metropolia consisted of pulling a piece of the track longitudinally (Figure 12) and bending the track piece (Figure 13) as it would bend when installed on a snowmobile with different force apply frequencies. The track piece measured is equivalent to what a half-track segment on Adams is. This means that in Adams the parameters must be 2 times what the results define.

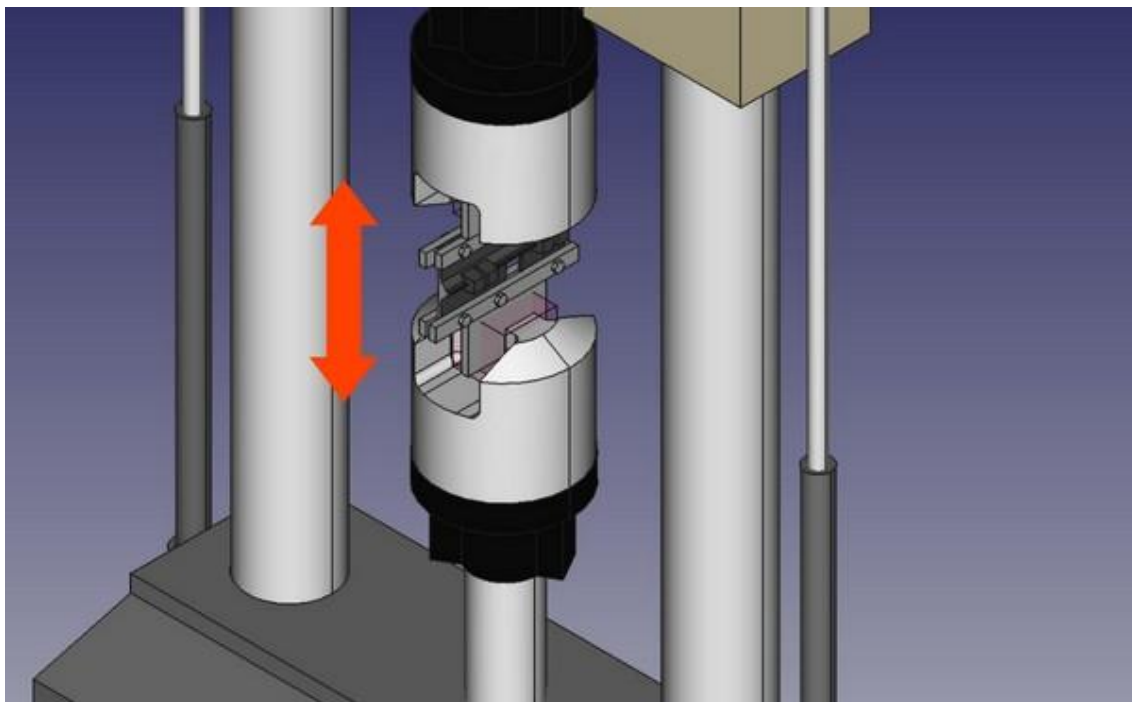


Figure 12. MTS 100 pulling a track piece longitudinally (Makkonen P. 2022).

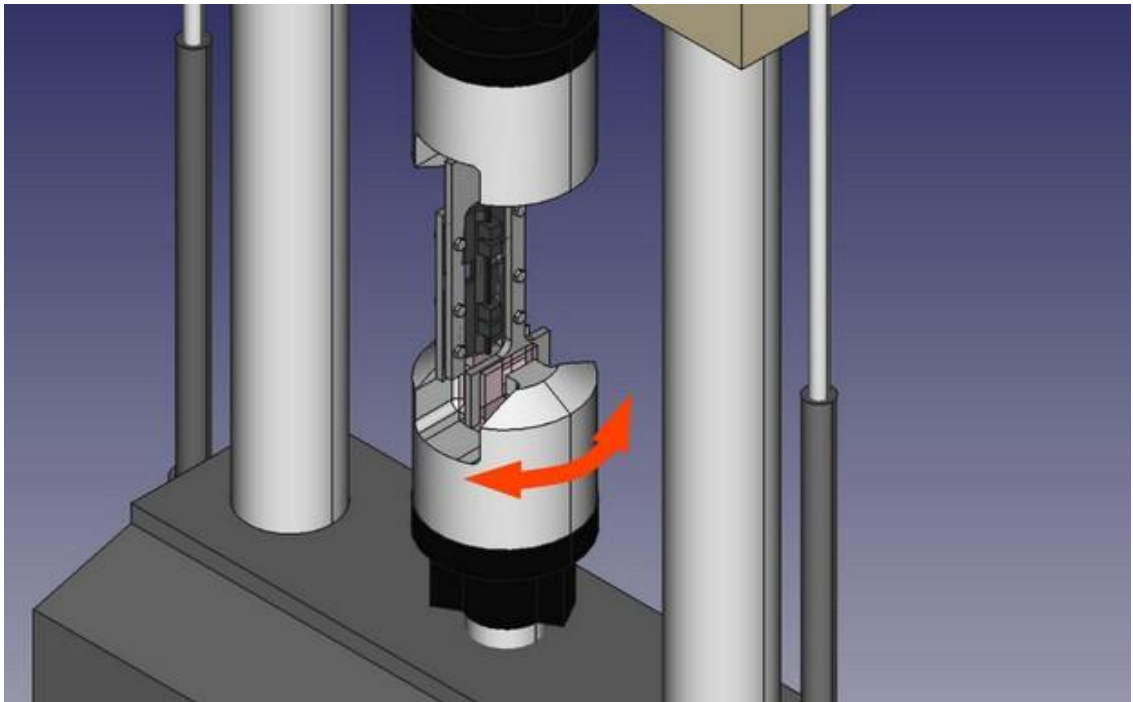


Figure 13. MTS 100 bending the track piece (Makkonen P. 2022).

In short Metropolia tested a track piece with these two setups straining it up to the point that the track was starting to break to find the maximum force/strain amount a track withstands. Strain amount suitable for the test was found to be 2 mm. They also defined when the track force–strain dependency acted linearly. After they defined the dynamic behaviour of the track with sweeping from 0 to 10 Hz with 0 to 2 mm strain and constant 0,2 Hz, 1 Hz and 5 Hz with strain from -1 to 2 mm.

The parameters defined by Metropolia tests (table 1):

Table 1. Track parameters as defined by Metropolia University of Applied sciences (Makkonen P 2022).

Half Belt Averages:									
Average	X-direction	Hz	p0	p1	p2	p3	p4	p5	c1
		0,05	-0,781895	5,70565	-0,71153	0,0534804	-0,0021466	1,8745E-05	1,7032775
		0,2	-0,55358375	1,03423	1,18790375	0,3589613	-0,241605	0,04698768	0,2495225
		1	-0,45063375	1,31457	1,4276375	0,3389793	-0,3089675	0,0702477	0,0568615
		5	-0,34515625	1,6774625	1,7044875	0,275428	-0,4029175	0,10668063	0,0133478
		0-10	0,04900505	1,7184177	905,7380087	-17,823495	-0,0561615	-0,0002412	-0,075852
	Average:		-0,41645274	2,29006604	181,8693015	-3,3593291	-0,2023596	0,0447387	0,3894315
	YY-direction	0,2	0,04900505	1,7184177	905,7380087	-17,823495	-0,0561615	-0,0002412	-0,075852
		1	0,05173157	0,3278294	1699,008911	7,482476	-0,6281338	-0,000299	-0,060012
		5	-0,00475242	2,330043	626,809938	-3,6944	0,02016938	0,00013459	-0,019552
		0-10	-0,000749567	0,8190561	-33,249662	16,17112	-0,0015617	0,000618	-0,003134
	Average:		0,023808658	1,29883655	799,5767988	0,5339254	-0,1664219	5,3097E-05	-0,039638
	YZ-direction		-0,000199659	1,0834721	18,9153	21,73481	0,01698248	0,00065112	-0,00144

On table 1 X–direction is the longitudinal measurements and YY direction is the bending direction measurements. K1-5 stiffness values shown in Figure 8 are the p values of the X–direction. Dampening is defined as c1 of the table 1.

At the time of this thesis written it is not possible to define the track with all the parameters that are measured. Non-linearity is possible to add only to longitudinal X stiffness parameter. It seems to be, though, the most important parameter for the model to stay stable during simulation. Track segment Y– and Z–directions are not defined, and the dampening does not behave correctly dynamically (c1 0,05 Hz values are not measured dynamically). As a general notion, an ATV model would be much more realistically defined with a steel track as rubber hysteresis and non-linear behaviour would not be affecting the model.

To tackle the problem with lacking non-linearity and parameters, parameters to use are the 5 Hz results for rotational stiffness and all the dampening definitions. Translational Y and Z direction stiffnesses and dampening could be defined as the same as X direction as they should not affect the model behaviour too much. This way the model should work somewhat accurately on average snowmobile driving speeds. It is also possible to simulate the model with different speeds and use the Hz value closest to the speed track is running. Higher driving speeds would require measurements with a different measurement device that is able to stress a segment piece with higher frequencies. With different measurement frequencies, frequency scaling may be added to the model.

4.2 Friction

When building an accurate model of the rear track/suspension system, frictions between parts are necessary to measure. For the minimization of energy consumption of the system, different usable material pairs should be measured for the simulations. This way differences in power/torque needed to run the system can be simulated.

Part pairs that have frictions between them are the track clip–track rail, the sprocket–track clip, the track–track rail and on some situations the supporting wheels–track. Static friction coefficient and dynamic friction coefficient should both be measured as some parts are moving (track clip- track rails) and some frictions that are present are static (sprocket–track clip). Joint frictions are needed to define if the model is run on terrain that causes force impulses to the system. If the track is driven free without ground contact, joint frictions are not needed. It is also likely that both the static and dynamic frictions are present i.e., during different phases of sprocket–track interaction

As the material friction measurement data is not available at the time of this thesis is being written, the frictions used for simulations are general table values of proper material pairs as an example from Adams internal manual.

5 ADAMS MODELLING AND THEORY

To understand the snowmobile model in Adams it is necessary to discuss how modelling in Adams Car with ATV-plugin is done. The snowmobile model is also necessary to study to understand the limitations and possibilities the model has. It is also important to understand how tracked vehicle theory discussed in chapter 3 is utilized in ATV.

5.1 Snowmobile structure

For a full vehicle snowmobile model to be the most convenient to build in Adams, it is split into 6 entities. These entities are the rear suspension, the drive sprocket, the track, the front suspension, the motor and the chassis. This thesis focuses on the rear suspension, the drive sprocket and the track combined entity as it is the combination of these entities that produce driving force of the vehicle and have most of the moving parts present. The chassis used with the model is an old chassis of an existing snowmobile model. Definitions of the model are presented in attachment 2.

The full vehicle assembly of the snowmobile in Adams is presented in Figure 14:

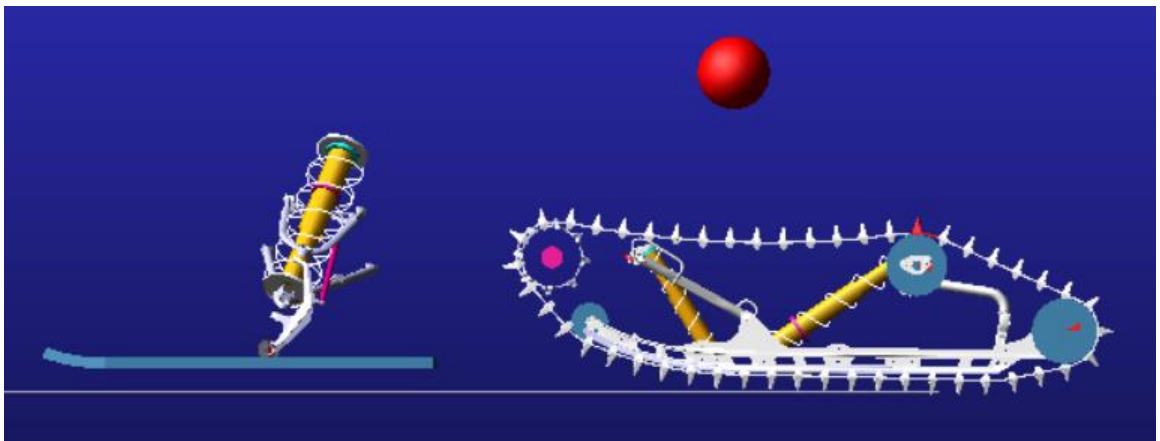


Figure 14. Full vehicle assembly of a snowmobile.

The red balloon presents the driver. Masses of chassis parts are present in the model on their designed positions and affect the simulation, but from Figures it is impossible to see anything useful accurately without zooming the rendering (Figure 15).

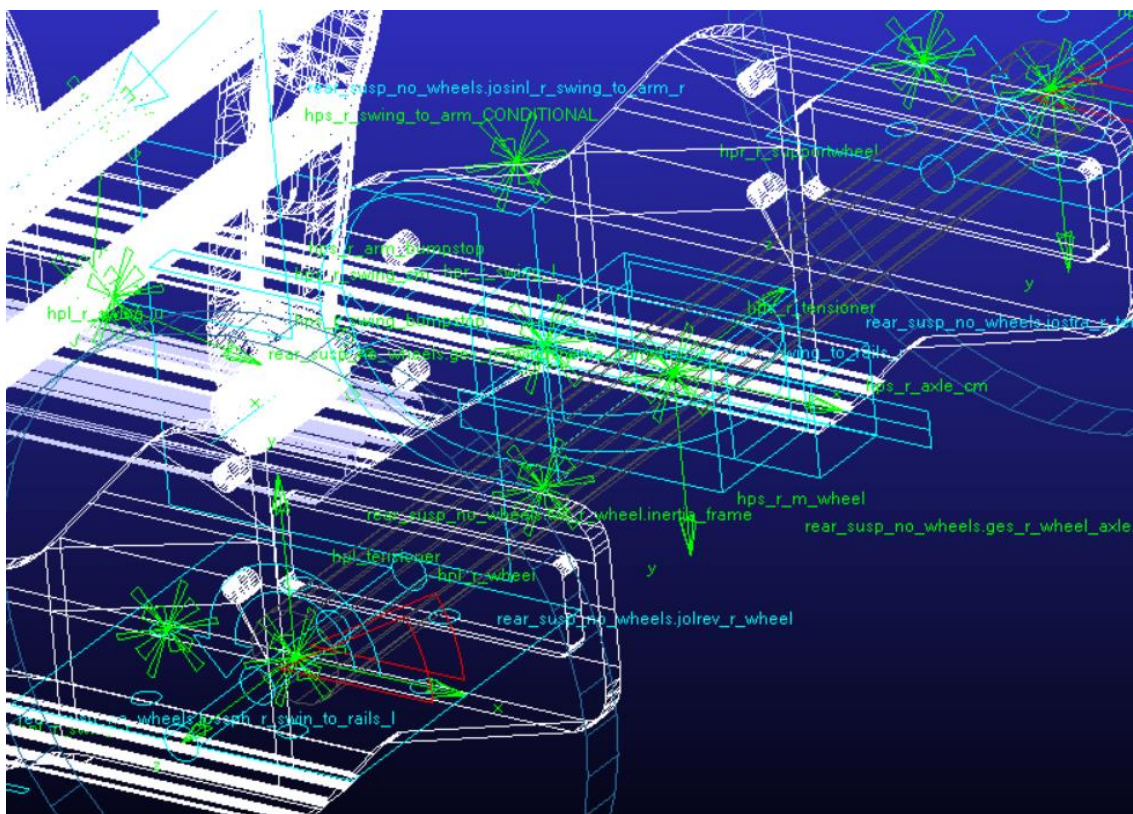


Figure 15. A wireframe rendering with close zoom.

Wireframe rendering allows user to see the hardpoints on designated positions and all the model parts and joints visually. Wireframe rendering allows user to visually explore that everything is in correct positions especially if using imported 3D-CAD graphics.

5.2 Modelling procedure

Adams modelling procedure starts with the templates. Templates are used to make complicated models such as a full vehicle modular and easily modified. As an example, a template could be a motor, a chassis, a front suspension or a track of a tracked vehicle. Modularity allows a designer to use existing templates for new products simulations faster. Templates can be defined exactly to the dimensions and parameters of a model to be simulated but usually they are only for general model structure. For example, McPherson suspension system is always the same as a structure, in general only dimensions and parameters such as suspension stiffness and dampening change from vehicle to vehicle. Therefore, one McPherson suspension template is enough for the designer to build several McPherson suspensions. The more exact definitions of a model are usually done at the subsystem level where it is not possible to make fundamental changes to the model as removing or adding joints.

In Adams template mode a model is first defined with the hardpoints. The hardpoints are used to define joints between parts, the dimensions of rigid or flexible parts and all the necessary data for an Adams model to function. They are usually the best to define to the centre of masses of the parts and joint the points of MBS. The hardpoints define markers that are needed for different requests, i.e., velocity request of a part.

After the hardpoints are defined properly, reference frames are defined to the hardpoints. A reference frame is a local x, y and z coordinate system that is used to rotate a part in the global coordinate system. It makes possible to define dimensions in the local coordinate system separated from the global coordinate system. It is not mandatory to add a reference frame to all the hardpoints, for example if a hardpoint is just a point for lining a part.

After the coordinate space has defined hardpoints and reference frames, user can start to add parts to the system. It is not possible to add parts without hardpoints as their position cannot be defined without. Parts are defined mass and inertias. Parts are then added geometry if the user wants to. Geometry can be imported, or the internal modelling of the program may be used for building a geometry. If part has a defined a geometry, Adams can calculate inertias and masses from it automatically after the material parameters are defined.

After all the parts for the template are defined, they are defined how they relate to each other. Relations are usually joints, suspensions, dampers, bushings, bump stops, rebound stops and forces. Relations restraint or force the movements of parts. With these definitions, the system should be modelled in a way that it is possible to achieve static equilibrium with a static simulation. It is however not mandatory to gain static equilibrium, Adams can start solving a problem with a dynamic solver instantly.

After a template is finished, it may be opened in Adams standard mode to make a subsystem. A subsystem is limited in a way that all the functions of the template mode are not present. Difference in a subsystem on the standard mode when compared to the template mode is that it can be simulated, or it can be used in an assembly of subsystems. As an example, a snowmobile full vehicle assembly could consist of a motor, a rear suspension, a track segment, a front suspension, a chassis and a sprocket subsystem and this assembly could be simulated as a full tracked vehicle assembly.

Before going to subsystem and assembly level templates must be defined how they would act in relation to other subsystems as a subsystem in the template mode. This is done with mount parts and communicators. Mount parts are ideal massless parts that allow building joints or other relations between subsystems in an assembly. For example, a joint can be defined between a wheel part and a mount part name on a wheel template. On other template (chassis) a mount part is then defined with an according name. When these templates are built as subsystems and then as an assembly, the wheel joint is automatically in the right place, if on both templates there is a proper communicator pair defined. The communicators request (input) or feed (output) data to other communicators with the same names on other subsystems. It is mandatory to have an output communicator pair for an input communicator for the model to be solvable, but output can be done without input as it only feeds data. If there is no input communicator for an output communicator, the data is irrelevant. (MSC 2021 c; MSC 2015 e)

5.3 Rear suspension entity

Snowmobile rear suspension–track structure is complicated structure which has several tasks for the proper functioning of the vehicle. The structure used in this project consisted of the drivetrain sprocket, the rear wheels, the supporting wheels, the front wheels, the rear arm wheels, the track, the front arm and rear arm, the front swing and rear swing and the front and rear spring–dampers. The drivetrain sprocket conveys power and torque to the track directly. The track then transmits power and torque to the driving surface that is usually snow, but there are some special cases such as driving on water during summer. The structure works also as suspension and as such it ensures the best possible surface contact, drive ability, safety and driving comfort. Figures of the rear suspension model are presented in Figures 16 and 17:

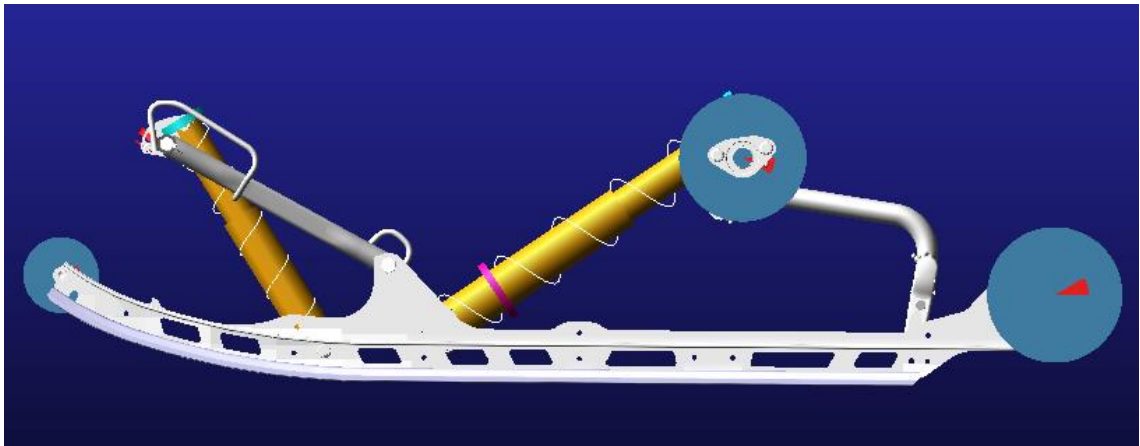


Figure 16. Sideview of the rear suspension subsystem.

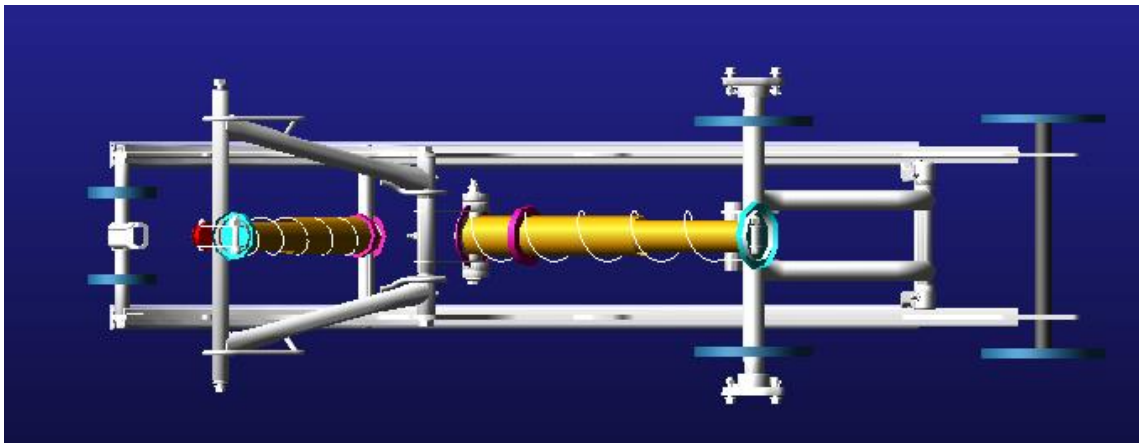


Figure 17. Top view of the rear suspension subsystem.

Figure 18 presents a snowmobile rear suspension assembly of the motor, the sprocket, the wrapped track and the suspension structure:

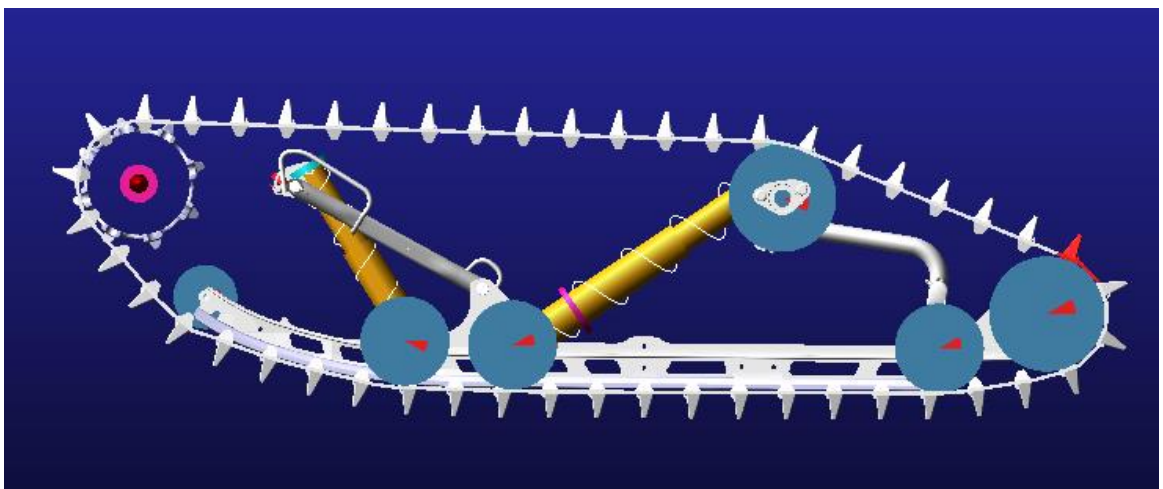


Figure 18. Snowmobile rear suspension entity assembly with a wrapped track.

5.4 Track

The track consists of track segments (Figures 19 and 20) that are wrapped around track holders. The track may be built using parametrized dimensions or imported graphics as in Figures 20 and 21 (MSC 2021 c; MSC 2015 e):

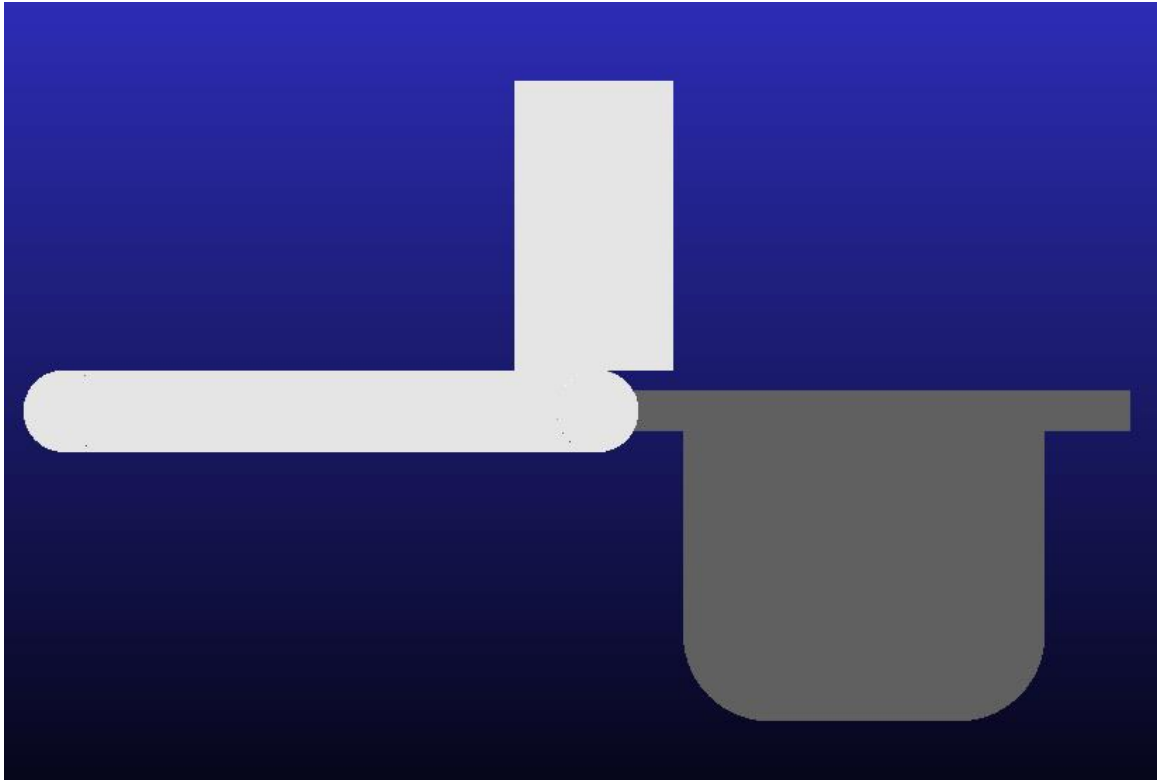


Figure 19. Parametrized track segment sideview.

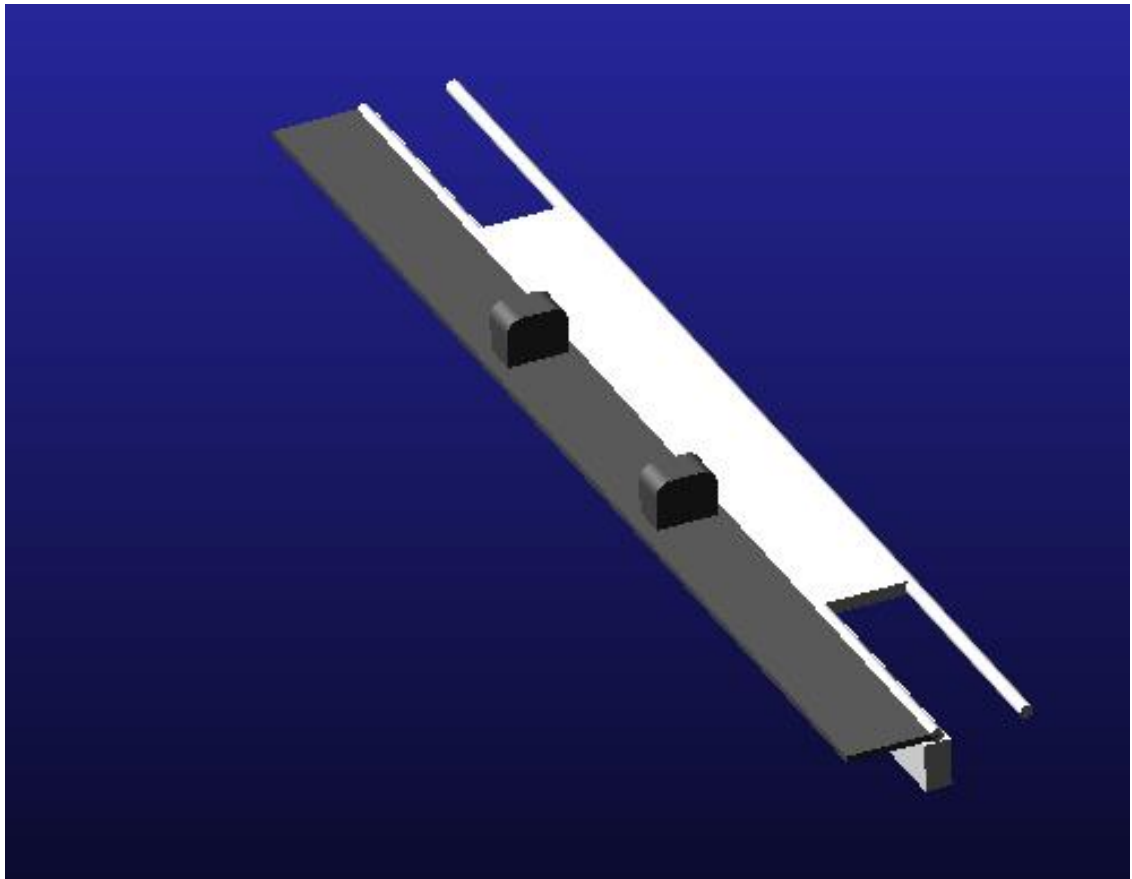


Figure 20. Parametrized track segment isometric view.

When using imported graphics, it is necessary to define the parametrized track segment dimensions for the Adams track wrapper to work properly. When building a track model, first should be built a parametrized track segment and confirm that it works properly. After the parametrized model works importing graphics is an option for more realistic contacts between the track and the suspension structure.

The track is built around track holders that are called trackwheels and track rails. The track modelling and track parts are special ATV-parts that come with ATV-plugin. The track segments are joined into a chain of track segments with Adams force FIELD function between each segment to build a complete track by the Adams track wrapper functionality. The track wrapper functionality follows a path defined by radii of track holders and the track rails. In practice, it adds segments after each other adding bushing element between every segment until the path ends to the first track segment and a full track is built. It is important to define track segment dimensions to fit track length defined by the wrapper. (MSC 2021 c, MSC 2015e)

FIELD function calculates forces as according to the Timoshenko beam model (the theory of the Timoshenko beam discussed further in 5.5) on the Adams solver. According to Adams internal user manual, FIELD applies translational and rotational action–reaction forces between 2 markers called I and J markers. These markers are the points where the segment joins another segment. When using a track FIELD needs a subroutine for calculating the non-linear behaviour of the track segment connection. Non-linear behaviour at Adams version 2021.2.2 is only possible to add in the segment connection longitudinal direction. Adams uses FIESUB subroutine to add non-linear behaviour to the connection. (MSC 2021 c)

With a snowmobile track there may be over 50 track segments and this causes the track model to be very demanding to calculate for a computer. Practically the track develops more points to calculate for the solver than the rest of the whole model. Figure 21 presents a wrapped track that consists of 48 track segments with imported CAD geometry.

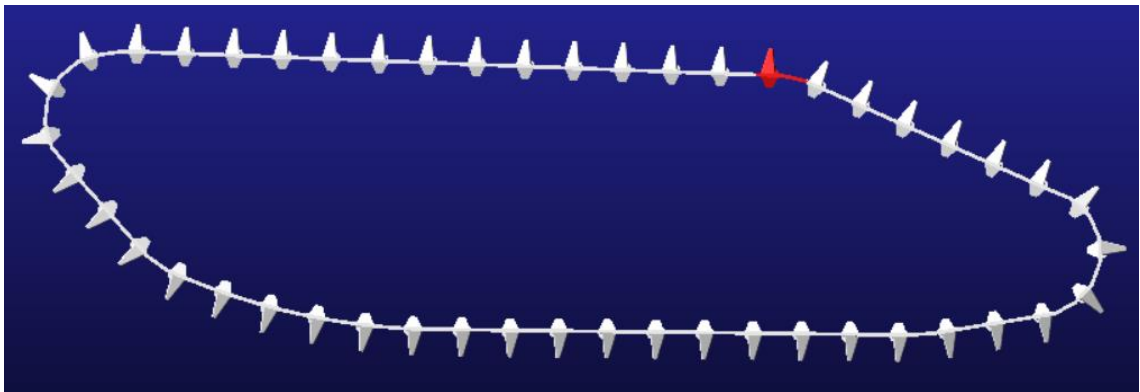


Figure 21. Wrapped track with rear suspension hidden.

For the FIELD function to work Adams needs 6x6 stiffness matrix (KMATRIX) and 6x6 viscous damping matrix (CMATRIX) defined between the I and J markers. In the KMATRIX translational and rotational stiffnesses are defined on local x and y and z axles and around them. CMATRIX is the according dampening matrix of the KMATRIX. CMATRIX can also be calculated as a ratio (CRATIO) of KMATRIX (MSC 2021 c). As discussed in chapter 3 the track links dynamic behaviour is most significantly defined by reaction and contact forces (Campanelli et al. 1998). This suggests that it is important to define KMATRIX and CMATRIX accurately. These stiffness and damping matrices are defined in the model using the laboratory measured values discussed in chapter 4. The track segment may be defined as to be modelled from 2 parts (segment and joint part) to

make it bend more realistically but in practice it does not add anything special to the model than more points to calculate.

5.5 Timoshenko beam model

Stephen Timoshenko and Paul Ehrenfest developed Timoshenko beam model to take in account shear deformation and rotational bending of a beam compared with Euler Bernoulli beam theory (Elishakoff 2019). When considering a track cut open from a position, attached from other end to a wall and let it hang free it acts as a beam that has very large shear deformation and bending. If only the bended shape of the track would be at interest, Euler Bernoulli beam would suffice for the problem at this state. The problem with Euler Bernoulli would be that when joining the cut parts back together as a track the edges would not be in correct shape, they would stay straight. With Timoshenko beam model the edges of the beam deform as shear deformation and rotational bending affect it the same way as a book with a great number of pages would deform under bending and because of this the shape of the beam will be more accurate. This is necessary when considering the track and how it is built. Without the deformation of the edges the built track would act stiffer than it should.

5.6 Drivetrain sprocket

The sprocket runs the track with teeth and knobs. Sprocket is designed in a way that initial contact is between the knobs but in situation more torque is needed sprocket tooth makes contact. Figures 22 and 23 present the sprocket from side view and front view with imported graphics. The geometry is simplified to optimize the model rendering so only the contact surfaces are presented. The pink round truss is the visualization of the parametrized motor that runs the sprocket. Figure 24 presents the sprocket definition example:



Figure 22. The sprocket sideview.

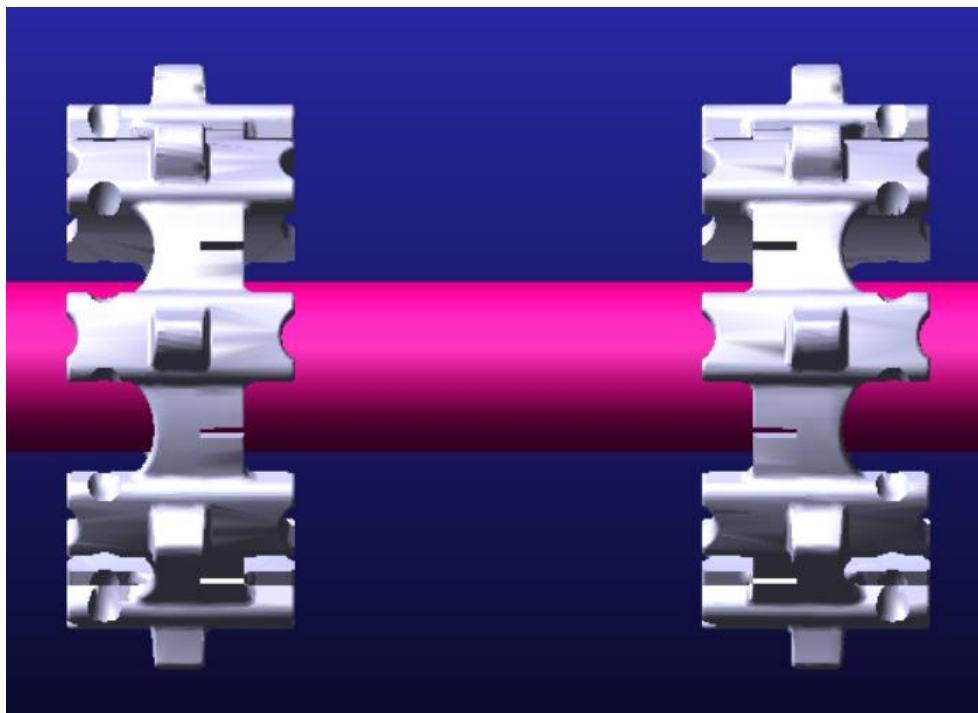


Figure 23. The sprocket front view.

Ad

Modify a Track Wheel

×



Track Wheel Name		.hhttest.sprocket.ues_sprocket	
Mass Properties		Geometry (User Entered) Contact	
Wheel Radius		92.0	
Wheel Width		380.615	
Number of Discs	2	Disc Distance	214.515
Number of Teeth		7	
Tooth Width	22.877	Tooth Height	13.598
Tooth Length	24.856	Flank Angle	19.6
Rotation Angle		128.0	Set
<input checked="" type="checkbox"/> Fix Rotation Angle			
Radial Contact		Track Segment Surface	
<input type="checkbox"/> Ground Contact			
 		OK	Apply
		Cancel	

Figure 24. Sprocket definition example.

The sprocket model is defined dimensions of the parametrized sprocket. Mass properties can be calculated according to the graphics by Adams. It is necessary to define the dimensions with imported graphics as the track wrapping procedure uses the parametrized sprocket dimensions (MSC 2021 c and 2015 e).

The contact between the sprocket and the track is defined using Adams CONTACT and IMPACT functions. Adams uses imported graphics for contact surfaces. Functions are further discussed in 5.7 and 5.8 (MSC 2021 c and 2015 e).

5.7 Impact function

The impact function defines if there is a collision between two objects. In practice this means that the Impact function calculates if two parts touch each other. Impact function is also used to define the damping coefficient between the objects as the damping coefficient is increased by the “depth” of the impact as the function of penetration variable. Impact is defined as function (20) (MSC 2021 c):

$$\text{IMPACT} = \begin{cases} \text{Max}(0, k(x_1 - x)^e - \text{STEP}(x, x_1 - d, c_{\max}, x_1, 0) * \dot{x} : x < x_1 \\ 0 : x > x_1 \end{cases} \quad (20)$$

Where: x is the expression of a distance variable ie. displacement between two markers

\dot{x} is the derivative of x

x_1 specifies free length of x

k is the stiffness of the surface interaction

e is exponent of the force deformation characteristic

c_{\max} is the maximum damping coefficient

d is the penetration value when maximum damping coefficient is applied.

When the x_1 is smaller than the x , there is no contact between the objects. When the x is bigger than the x_1 , there is contact existing and contact force is calculated then calculated. Figure 25 presents an impact situation with the track and the sprocket.

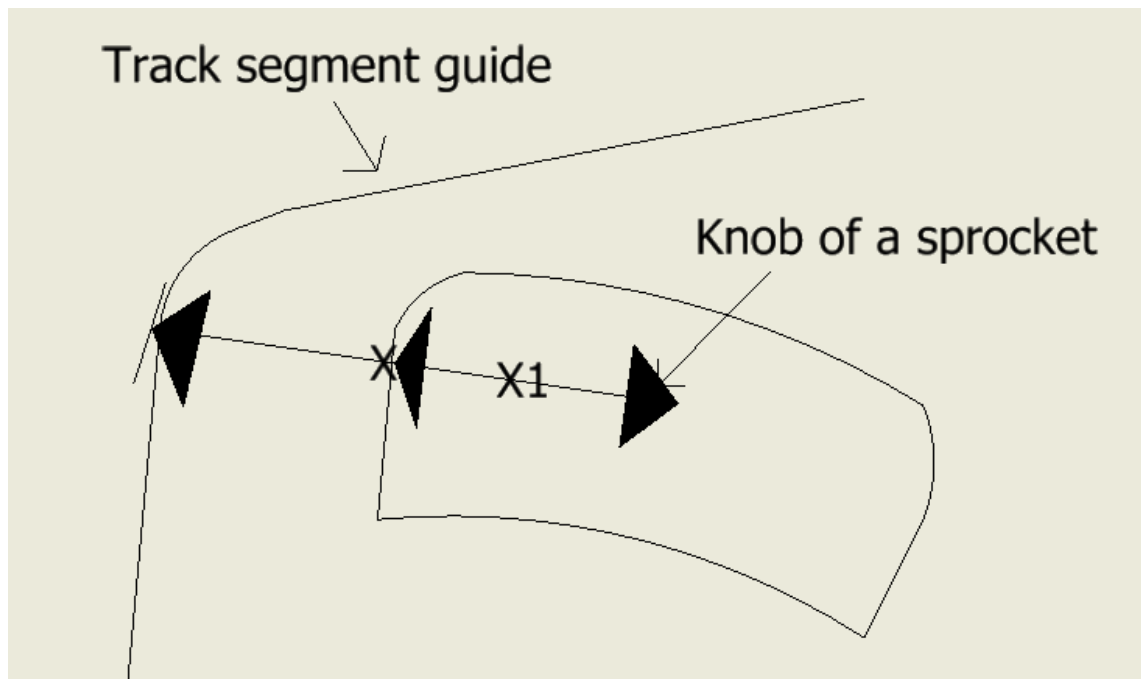


Figure 25. Knob of a sprocket before impact.

5.8 Contact function

The contact function defines forces between 3 dimensional or 2 dimensional objects if there is penetration between the objects. This means that contact is calculated if Impact function defines impact to be on. The contact function is used to add coulomb friction between the objects impacting each other. Static coefficient of friction and dynamic coefficient of friction are defined with the so-called friction transition velocities. The friction transition velocity defines velocity between contacting surfaces when the friction coefficient is completely dynamic friction coefficient. Stiction transition velocity defines the speed between contacting surfaces when the static friction coefficient reaches its maximum (MSC 2021 c). Figure 26 presents an example situation how the vector normal are understood by Adams from solid surfaces and how the friction between contacting surfaces is then calculated with outward vector normal defining the normal force directions used for friction calculations. Knob approaches track segment guide (red), and the impact function is 0. When the impact function reaches > 0 value the contact is on (green), and contact force calculation starts. The outwards normal vectors define the directions of the contact forces and slip velocity used for friction calculations.

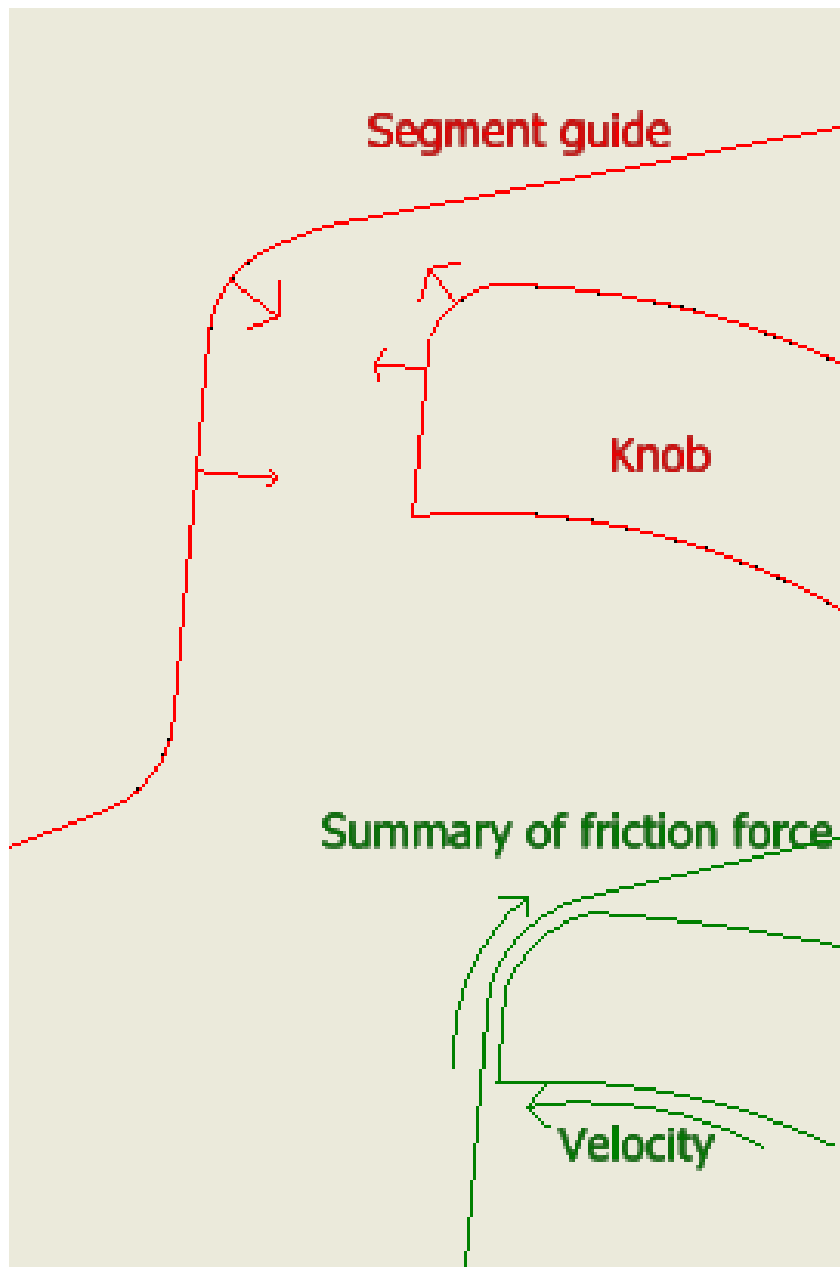


Figure 26. Knob–track segment guide contact.

5.9 Motor

The motor of the model is a simple parametrized torque–velocity dyno that runs the sprocket. It can be run with several methods as with user defined function. One of the simplest ways to run the model is using a velocity–torque dependency with a step function. The dyno is defined a velocity or torque it tries to reach and the other variable is then calculated by Adams accordingly. The simple dyno used on the model is a step function. Step function is defined as command “step(x, x1, h1, x2, h2)” and it builds a two–axis plot. x is an independent variable that can be a function Adams has. x1 is the

starting value of longitudinal axis, h1 is the first horizontal value, x2 is the last longitudinal axis value and h2 is the last horizontal axis value. The step function advances towards the h2 value from h1 value with constant x increase from x1 to x2. The h increase is at first smaller, then its linear and in the end, it decreases again to form a smooth curve (MSC 2021 c). For example, a torque dyno motor that accelerates in 5 seconds to 70 Nm torque would be defined with step function “step(time,0,0,5,70)”.

The model validation is easy to do with speed–torque measurements with a real snowmobile as velocity–torque graph of the model can be compared with a real snowmobile torque–speed data. Figure 27 presents a dyno defined with torque request and step function.

Ad Modify Dyno [X]

Dyno Name	.motor_test_nowheels_tracktest.power
Dyno Type	Torque
Function Type	User-Entered
User-Entered Function	
30000*step(time,0.5,0,2.5,1)	
Mean Value	100.0
Active	<input checked="" type="radio"/> On <input type="radio"/> Off
Geometry Scaling	15
<input type="button" value="OK"/> <input type="button" value="Apply"/> <input type="button" value="Cancel"/>	

Figure 27. Defining a random motor.

Adams has a more advanced velocity control system (Figure 28) for a simulated tracked vehicle as the Velocity Controller function. The velocity controller is defined maximum power, torque and brake torque of the motor and effective radius of the track going around the sprocket. It may be also defined revolte limiter for situations as when the track loses ground contact and cut off frequency, so the motor avoids enhancing vibrations present in the track system. The velocity controller may be defined to try to reach certain constant speed for the vehicle or user defined speed function.

Ad

Modify Velocity Controller

×

Velocity Controller Name	<input type="text"/>
Velocity Input	<input checked="" type="radio"/> Constant <input type="radio"/> Function
Velocity Function	<input type="text"/>
P Gain	<input type="text"/>
I Gain	<input type="text"/>
Cutoff Frequency	<input type="text"/>
Maximum Power (kW)	<input type="text"/>
Maximum Engine Torque	<input type="text"/>
Maximum Brake Torque	<input type="text"/>
Effective Radius	<input type="text"/>
Activate Rev. Limiter	<input checked="" type="radio"/> On <input type="radio"/> Off
Max. Angular Velocity	<input type="text"/>
Use Initial Step	<input checked="" type="radio"/> Yes <input type="radio"/> No
Initial Velocity	<input type="text"/>
Step Start Time	<input type="text"/>
Step End Time	<input type="text"/>
Symmetric	<input checked="" type="radio"/> Yes <input type="radio"/> No
Active	<input checked="" type="radio"/> On <input type="radio"/> Off

Figure 28. Velocity controller.

5.10 Front suspension

The front suspension entity is presented in Figure 29.

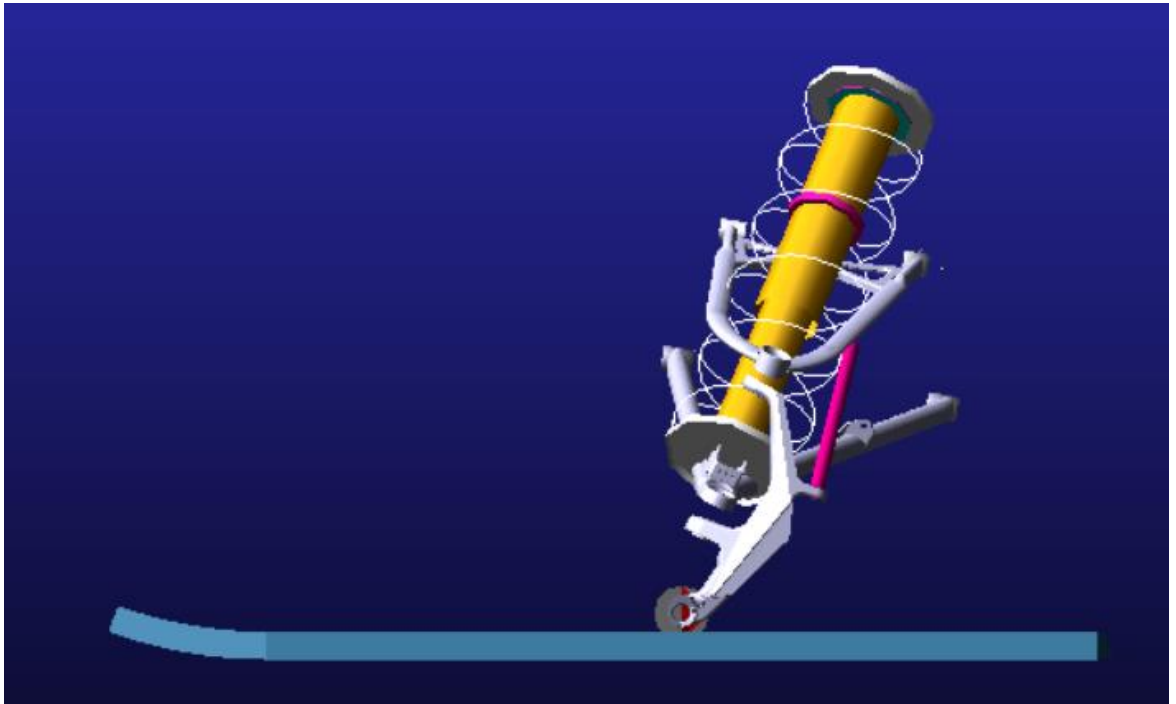


Figure 29. Front suspension entity.

It consists of two skis, two spring–dampers, two bushings, suspension arms and ski legs. The skis may be replaced with wheels for model validation purposes (Figure 30).

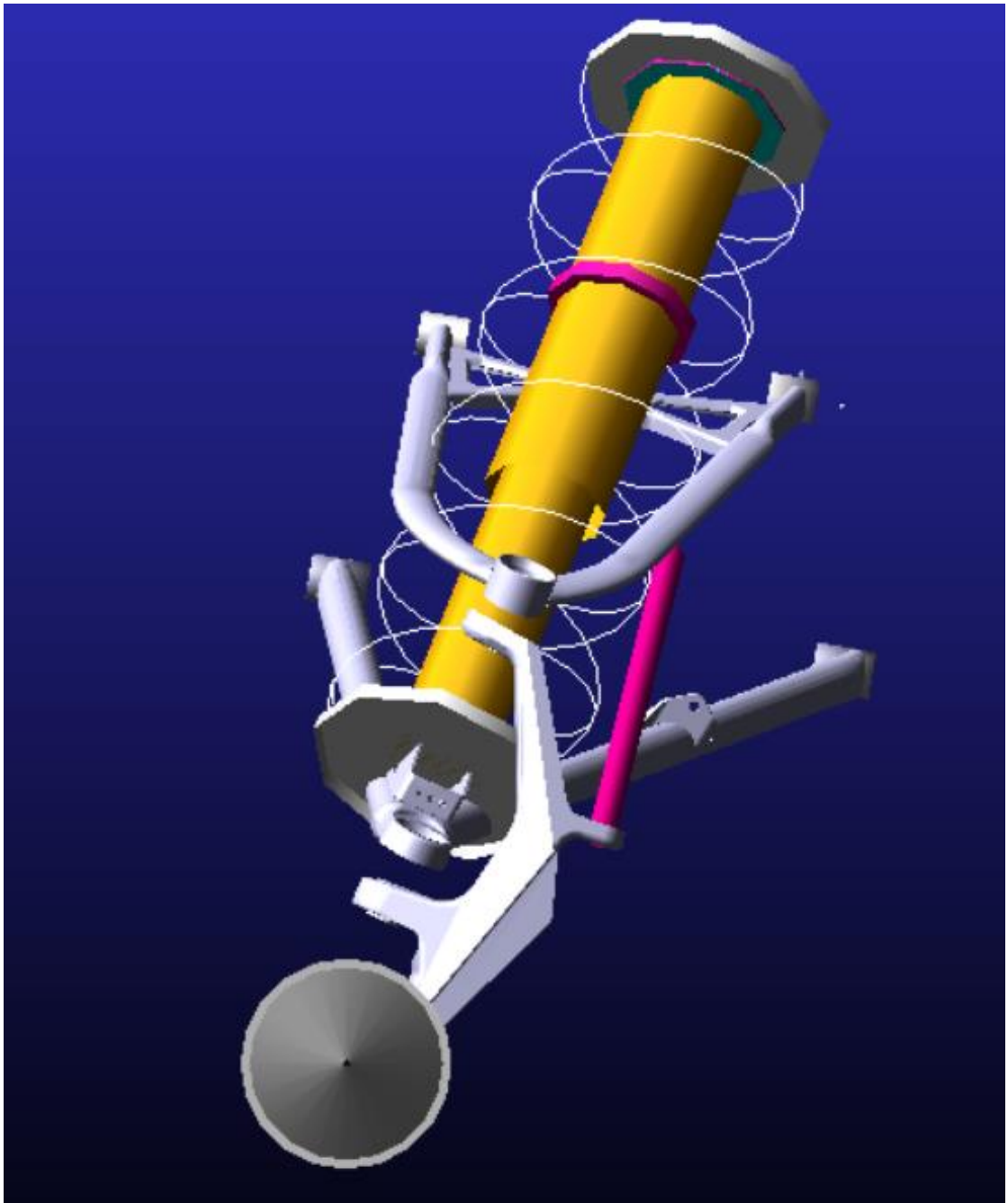


Figure 30. Front suspension with wheels.

5.11 Chassis

The chassis is presented in Figure 31 as a mass point coordinate system.

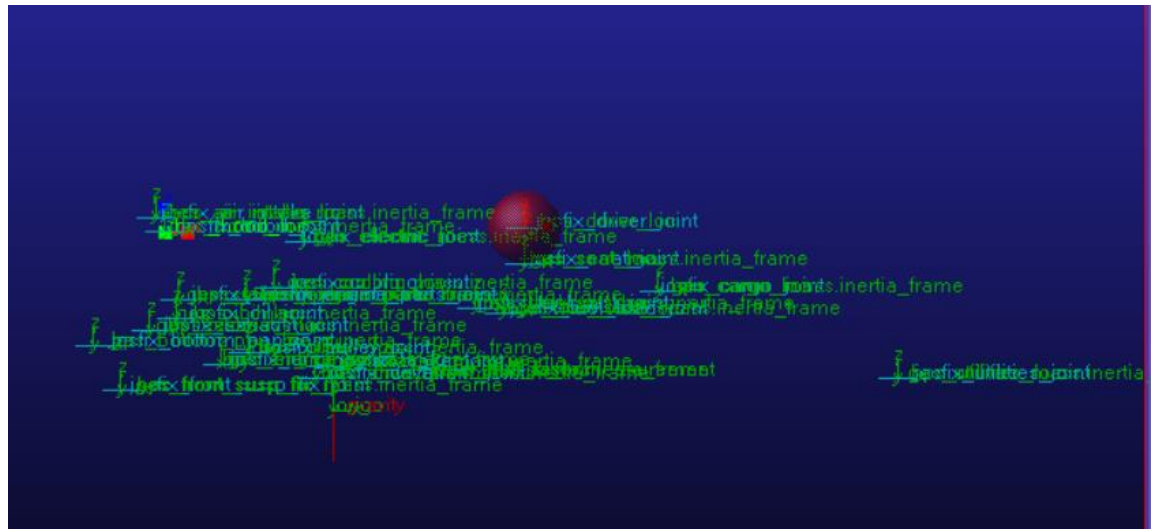


Figure 31. Snowmobile chassis.

It consists of several mass points of different snowmobile parts with proper inertias. The chassis is mounted with mount parts to the rear suspension entity, motor and front suspension. The chassis is not built for this simulation model separately, but it is an existing chassis subsystem of a snowmobile.

5.12 Adams Car hard road

The hard road feature on Adams Car is used to build a drive terrain for a vehicle without the soft soil theory. This means that only the friction developed by contact surfaces can be used as a tractive effort force. In practice the hard road calculates contact as with any other contact on the model. Adams Car hard road feature works with tracked vehicles and it is used with model validation in this thesis. The hard road is basically 3D solid geometry. The hard road may be built to have slopes and bumps and ditches to present real terrain (MSC 2021 c). For validation purposes the road must be presenting a driving surface that has been driven for the validation measurements. Figures 32 and 33 present dry asphalt hard road definitions that are used in the validation simulations.


```

$-----MDI_HEADER
[MDI_HEADER]
FILE_TYPE      = 'rdf'
FILE_VERSION    = 5.0
FILE_FORMAT     = 'ASCII'
(COMMENTS)
{comment_string}
'ADAMS Tracked Vehicle Toolkit - Flat road'
$-----UNITS
[UNITS]
LENGTH         = 'meter'
FORCE          = 'newton'
ANGLE          = 'radians'
MASS           = 'kg'
TIME           = 'sec'
$-----MODEL
[MODEL]
METHOD         = '3D'
$-----OFFSET
[OFFSET]
X              = 0.0
Y              = 0.0
Z              = -0.81
$-----NODES
[NODES]
NUMBER_OF_NODES = 4
{ node   x_value   y_value   z_value }
  1  -100.0  -100.0   0.0
  2  -100.0   100.0   0.0
  3   100.0  -100.0   0.0
  4   100.0   100.0   0.0
$-----ELEMENTS
[ELEMENTS]
NUMBER_OF_ELEMENTS = 2
{ node_1  node_2  node_3  mu }
  1     4     2     1.0   1.0
  1     3     4     1.0   1.0

```

Figure 32. Road geometry datafile.

```

$-----MDI_HEADER
[MDI_HEADER]
FILE_TYPE      = 'spf'
FILE_VERSION    = 1.0
FILE_FORMAT     = 'ASCII'
(COMMENTS)
{comment_string}
'This file contains the Hard Soil parameters originally from the'
'msc_0001.spf file'
'Ex of materials equivalent to the stiffness in this file:'
'Materials Asphalt (E = 2500 N/mm**2 and nu = 0.35)'
'and Rubber (E = 25 N/mm**2 and nu = 0.3)'
'and geometry radius R = 36 mm'
'Using Hertzian Contact Theory to estimate contact stiffness'
'would result in k = 2E+02 N/mm = 2E+05 N/m'
$-----UNITS
[UNITS]
LENGTH         = 'meter'
ANGLE          = 'radians'
FORCE          = 'newton'
MASS           = 'kg'
TIME           = 'second'
$-----HARD_PARAMETERS
[HARD_PARAMETERS]
STIFFNESS      = 200000.0
DAMPING        = 2000.0
EXPONENT       = 2.0
PENETRATION    = 0.001
STATIC_FRICTION      = 0.9
DYNAMIC_FRICTION    = 0.7
STICTION_TRANSITION_VELOCITY = 0.1
FRICTION_TRANSITION_VELOCITY = 0.5
STIFFNESS_VALIDATED_LENGTH_UNIT = 'mm'

```

Figure 33. Soilproperty datafile.

5.13 ATV soft soil

ATV has soft soil function for modelling the track–terrain interaction with deformable terrain. The soft soil model is very important to have proper parameters as it affects the track sinkage and tractive effort of the vehicle. ATV soft soil model is based on Wong, Bekker, Janosi, Hanamoto and Terzaghis work discussed in chapter 3. The soft soil road is built with the soil property file that defines the soil properties and the road data file that defines the size of road. The road is presented as ATV regular grid. Practically the grid consists of rectangle segments that are used to calculate their deformation according to the terramechanics theory discussed (MSC 2021 c; MSC 2020 b; MSC 2015 e). The deformation can be visually presented if the user wants. Figures 34 and 35 present an example of how the soft soil is defined in Adams.

Hard Soil		Soft Soil		File Units	
Soft Soil Routine					
<input type="radio"/> Legacy (Type 1) <input checked="" type="radio"/> Standard (Type 2) <input type="radio"/> User					
General Parameters				Shear Equation Type	
				<input checked="" type="radio"/> 1 <input type="radio"/> 2 <input type="radio"/> 3	
Specific Weight		3000.0		Longitudinal Parameters	
Internal Shearing Active		<input type="radio"/> Yes <input checked="" type="radio"/> No		Cr Longitudinal	
Bulldozing Active		<input checked="" type="radio"/> Yes <input type="radio"/> No		PHlr Longitudinal	
Side Force Active		<input type="radio"/> Yes <input checked="" type="radio"/> No		Kr Longitudinal	
				Ci Longitudinal	
				PHli Longitudinal	
				Ki Longitudinal	
Vertical Parameters				Lateral Parameters	
Kc		6160.0		Cr Lateral	
Kphi		1.4935E+05		PHlr Lateral	
n		1.53		Kr Lateral	
K0		0.0		Ci Lateral	
Au		4.0E+07		PHli Lateral	
Cc		1.0E-05		Ki Lateral	

Figure 34. Softsoil parameter setup.

Vertical, longitudinal and lateral material behaviour parameters are defined. Shear equation type is defined.

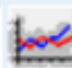




Road Setup		Save and Reload	
Soil Property File	mdids://atv_shared/soil.tbl/ms		 
Hull Soil Property File			 
Road Data File			
Road Reference Loc.	0.0, 0.0, 0.0		Read and Set
Road Reference Ori.	0.0, 0.0, 0.0		
Road Properties			Load Defaults
Road X Limits			
Road Y Limits			
Road Segment Numb			
Filter Factor	0.0		
Filter Level	0.0		
<input checked="" type="checkbox"/> Create/Modify Road Geometry from Road Data shl-file			

Figure 35 Softsoil setup.

In short, the ATV softsoil track–terrain interaction is simulated in next steps, when using shear equation 1 setting on Adams. Shear equation 1 setting is suited for dry fresh snow:

1. Vertical force per track segment is defined with (5). Road deformation is calculated on every track segment 8 times on the centres of track segment areas
2. Force direction of the vertical "Bekker" force is calculated with road and track segment normal as a vector: $\bar{u}_{force} = 0.5\bar{u}_{road} - 0.5\bar{u}_{segment}$.
3. (15) is utilized and the pressure on affecting a grouser calculated
4. Shear stress and shear displacements are defined with (9) and (10). If bulldozing is not on as (17) defines (18) is utilized
5. Grouser side wall thrust is added with (19)
6. Grouser force is calculated with (16) and summarized
7. Hull contact is calculated the same way as steps 1–4

(MSC 2020 d).

If the soil is frozen snow, shear equation type must be chosen as option 3. In this situation (10) is replaced with function (21) (MSC, 2020 d):

$$\tau = \tau_{max} \cdot K_r \left[1 + \left[\frac{1}{K_r(1-1/e)} - 1 \right] e^{1-j/K} \omega \right] [1 - e^{-j/K} \omega] \quad (21)$$

Where: K_ω is the shear displacement j on shear stress peak,
 K_r is the fraction of the shear at which the curve falls off towards.

As a snowmobile may be driven on different snow terrains simulations need to be done with the best suited shear equation model (1 or 3). Shear stress model type 2 is built for muskeg (swamp) drive terrain and therefore not discussed further in this thesis. It is also possible to add user written subsoil track routine to build a completely custom soft soil model.

The most demanding part with ATV soft soil simulations seems to be accurate soft soil data. With a snowmobile, terrain is usually snow and as discussed before snow is not exactly homogenous on different occasions. Because of this the simulations done with the model are recommended to do with parameters representing different snows and preferably parameters defined with bevameter tests.

6 SIMULATIONS

Simulations with the model are run with two main types. The first type is to simulate only the rear suspension entity (motor, sprocket, rear suspension and track) without terrain contact. This type of simulation represents the snowmobile track raised from the ground into the air. The rear suspension entity is fixed in position of the 3D space. With this type of simulation variables to the simulation are limited only to the internal motion resistances of the rear suspension entity and the model is faster to simulate as there is less variables needed to compute compared to a full vehicle model with drive terrain. Figure 36 presents the type 1 simulation assembly.

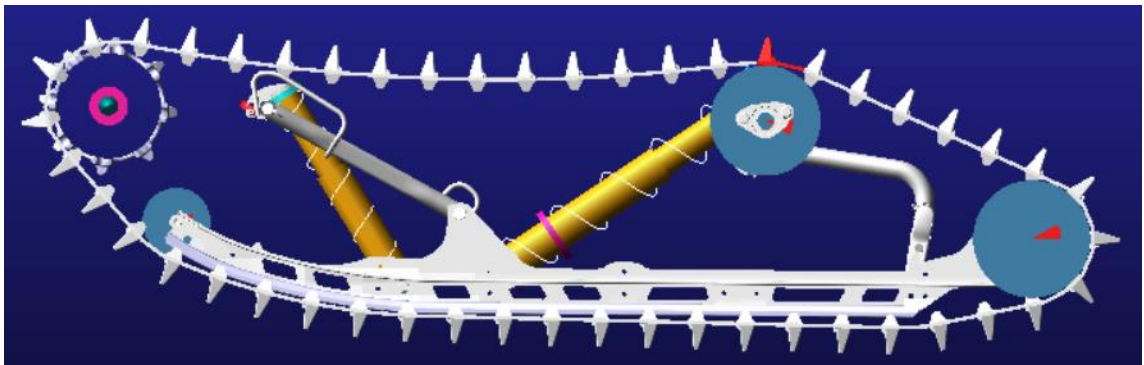


Figure 36. Type 1 simulation assembly.

Type 2 simulation assembly (Figure 37) presents the snowmobile as a full vehicle assembly consisting of the front suspension, the rear-suspension, the sprocket, the motor, the track and the chassis subsystems. In the simulations skis are replaced by wheels

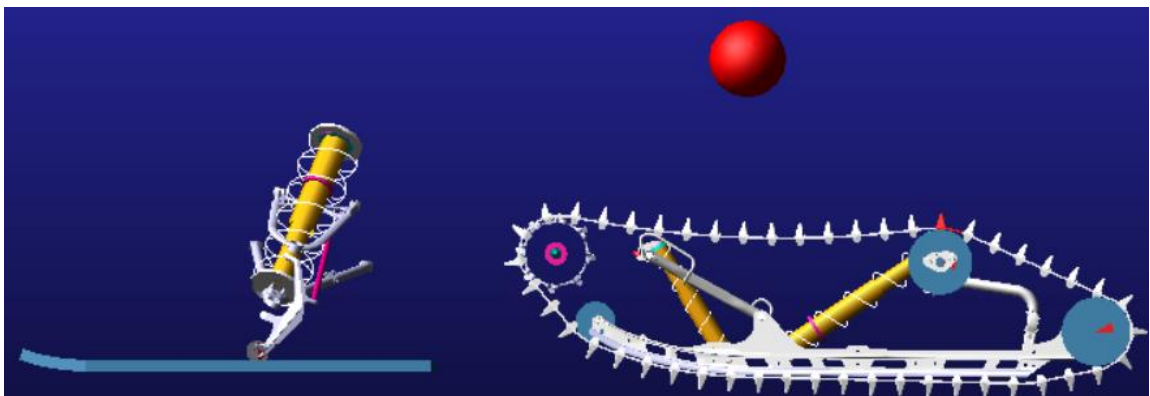


Figure 37. Type 2 simulation assembly.

This type of simulation needs terrain contact defined as the full vehicle model is not fixed in position of the 3D space. The terrain contact is presented with Adams Car hard road or ATV soft soil added. With track–terrain interaction added the computational effort demanded on the simulations is higher.

The model may be used after validation for the two main types of simulations with changing the sprocket to a different type of sprocket, changing track wheel sizes, changing the track and changing the friction of the track rail to represent different material pairs. The track wheels can be added or removed for different configurations. With the full vehicle simulations, the skis may be changed to different skis and for some validations skis may be replaced with wheels. Changing the track demands measurements to define the track stiffness and dampening values. Track measurements should be done with different tracks to define the best track for a snowmobile considering motion resistance optimization and to allow the model to be as exact as possible.

To validate the model, torque and angular velocity curves are convenient to compare for a certain vehicle run speed. Model validation is done with 3 type 1 simulations (10, 25 and 50 km/h) and 1 type 2 simulation (25 km/h on asphalt with wheels replacing skis). The results are compared with the measured results of a snowmobile to see if the simulated model behaves close to a real snowmobile

The computer used for validation simulations has Intel Core i7–7700HQ CPU and simulations are run with 8 threads. Simulation run times varied from approximately 8 to 24 hours depending on the type of simulation.

7 RESULTS

Measured torque demand for a snowmobile with the track on air with 10 km/h run speed is presented in Figure 38. Figure 39 presents the according simulation result on Adams.

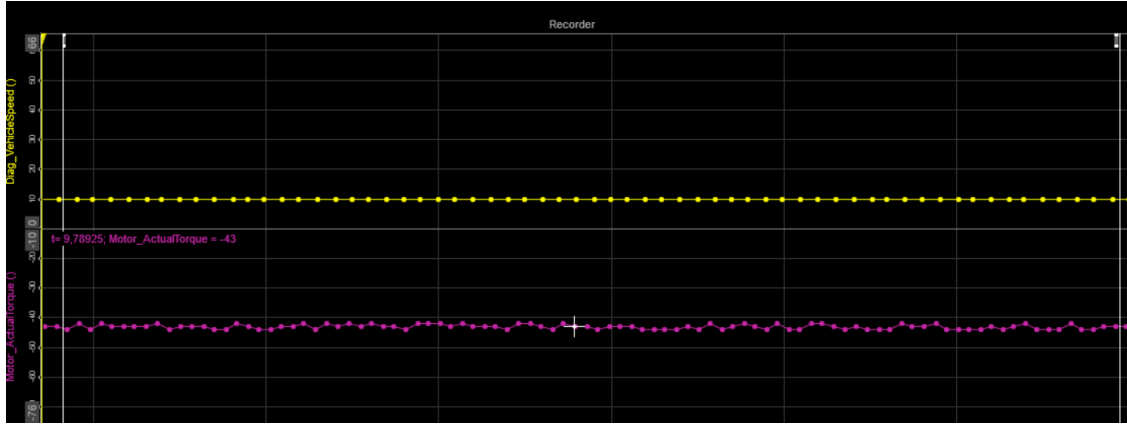


Figure 38. Measured data example.

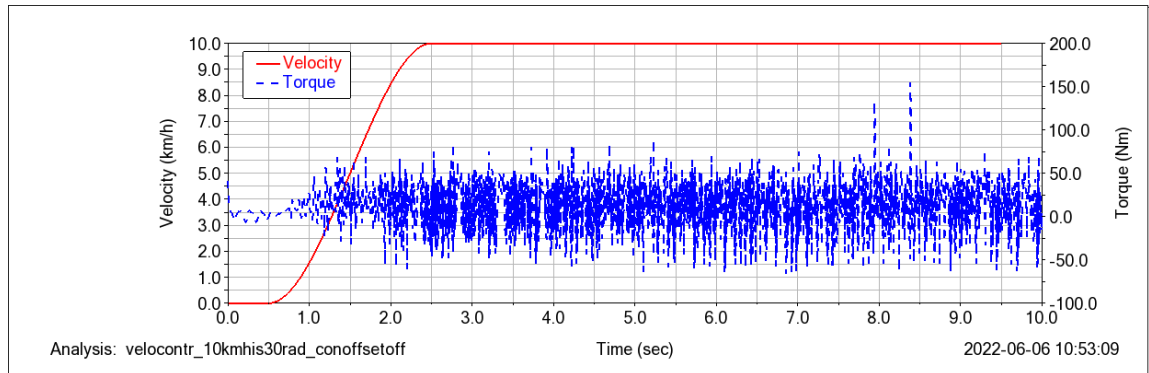


Figure 39. Simulated data example.

The measured data and Adams results are exported to Matlab for evaluation (Matlab code used is presented in attachment 3). The velocity unit used on the Adams model for the motor is angular velocity (degrees/second) and torque is Newton millimetres. Therefore, the results are modified to km/h and Nm units. The sprocket has 92 mm radius and as the circumferential speed of a point on edge of a circle is defined with function (22) the speed of the vehicle is the speed calculated by function (22):

$$V_t = \omega * r. \quad (22)$$

As torque in the Adams model is Nmm the simulated torque is shared with 1000 to have Nm as a result.

The measured torque is measured before transmission. The snowmobile gear ratio is 2,9 and transmission efficiency is determined to be 95 % by the designer of the transmission. Therefore, torque on the sprocket is calculated with function (23):

$$T_R = R_G * T_A * \eta \quad (23)$$

Where: T_R is the torque running the sprocket,
 R_G is the snowmobile gear ratio,
 T_A is the measured torque,
 η is the efficiency of the transmission.

Simulation type 1 consists of only the rear suspension entity, and it simulates a situation where the track is run on air. Simulation type 2 consists of a full vehicle snowmobile model, and it simulates a situation where the snowmobile is run on asphalt with skis replaced by wheels. Simulation types are further discussed on chapter 6.

7.1 Type 1 10 km/h

The simulated average torque data used is from 6–9 seconds of simulation time. 10 km/h simulation results are presented in Figure 40.

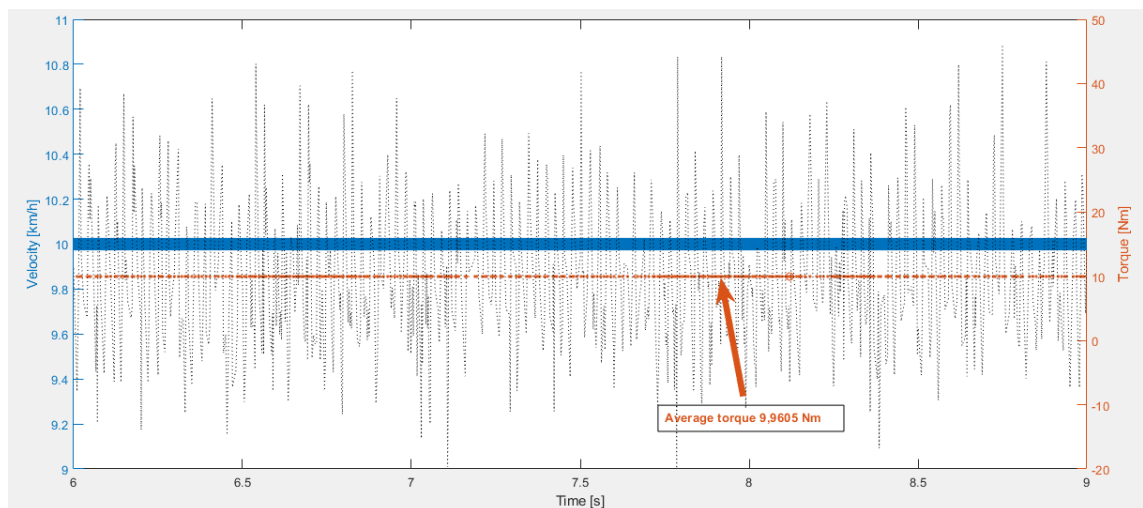


Figure 40. Type 1 simulation 10 km/h.

The average torque is presented with the orange line. Velocity is presented with the blue line. Raw unedited torque data is presented with the black dotted line.

7.2 Type 1 25 km/h

The simulated average torque data is presented from 6–9 seconds of simulation time. 25 km/h simulation results are presented in Figure 41. Figure 42 presents the average measured torque and measured torque with 25 km/h velocity.

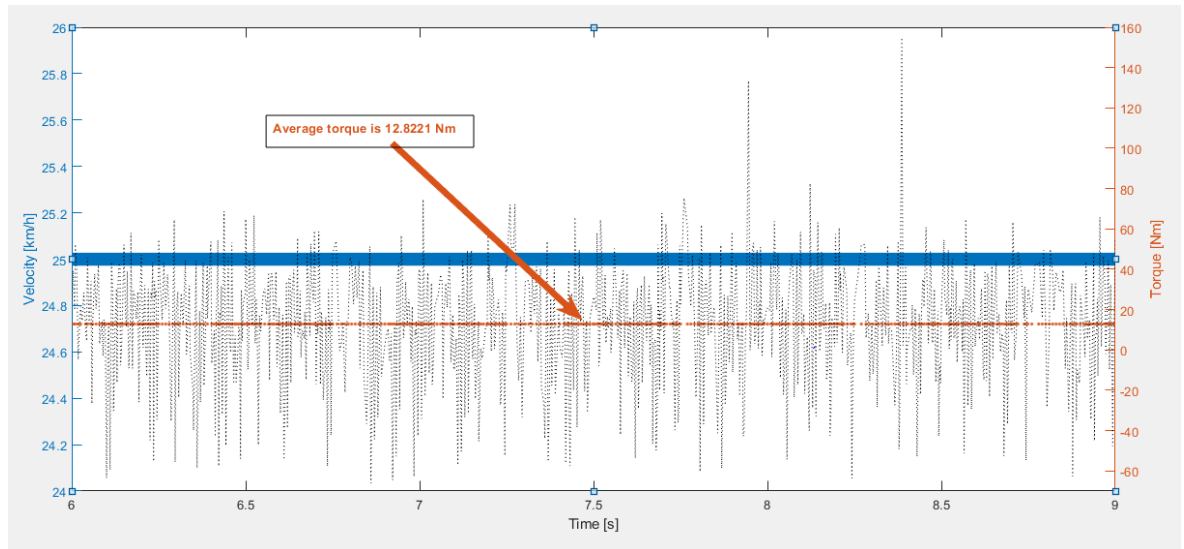


Figure 41. Type 1 simulation 25 km/h.

Figure 42 presents the results of 25 km/h and 10 km/h measured and simulated mean torques.

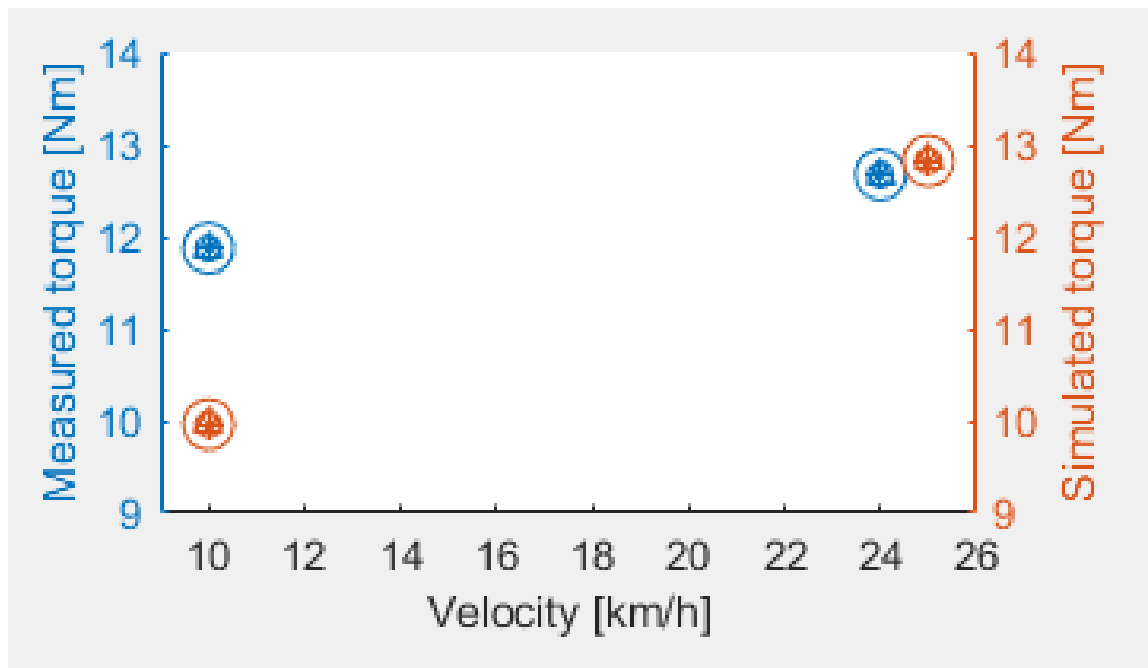


Figure 42. 25 km/h measured torque vs simulated torque.

7.3 Type 1 50 km/h

The simulated torque of a snowmobile with 50 km/h velocity is presented in Figure 43. Matlab's results are not presented as the model was not stable and able to run further and stable speed was not reached.

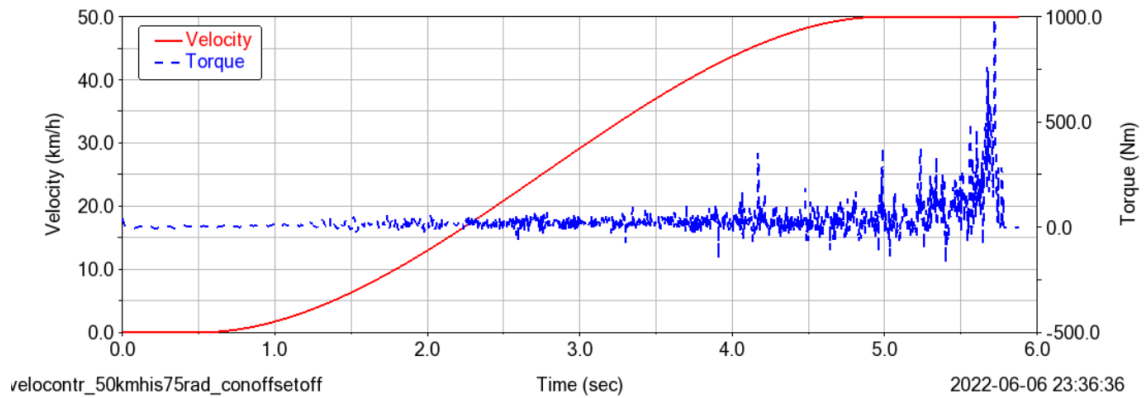


Figure 43. Type 1 simulation 50 km/h.

7.4 Type 2 20 km/h

Measured data (Figure 44) is from an old existing measurement of a different snowmobile. Type 2 validation simulation is made on the hard road with skis replaced by wheels (results are presented in Figure 45).

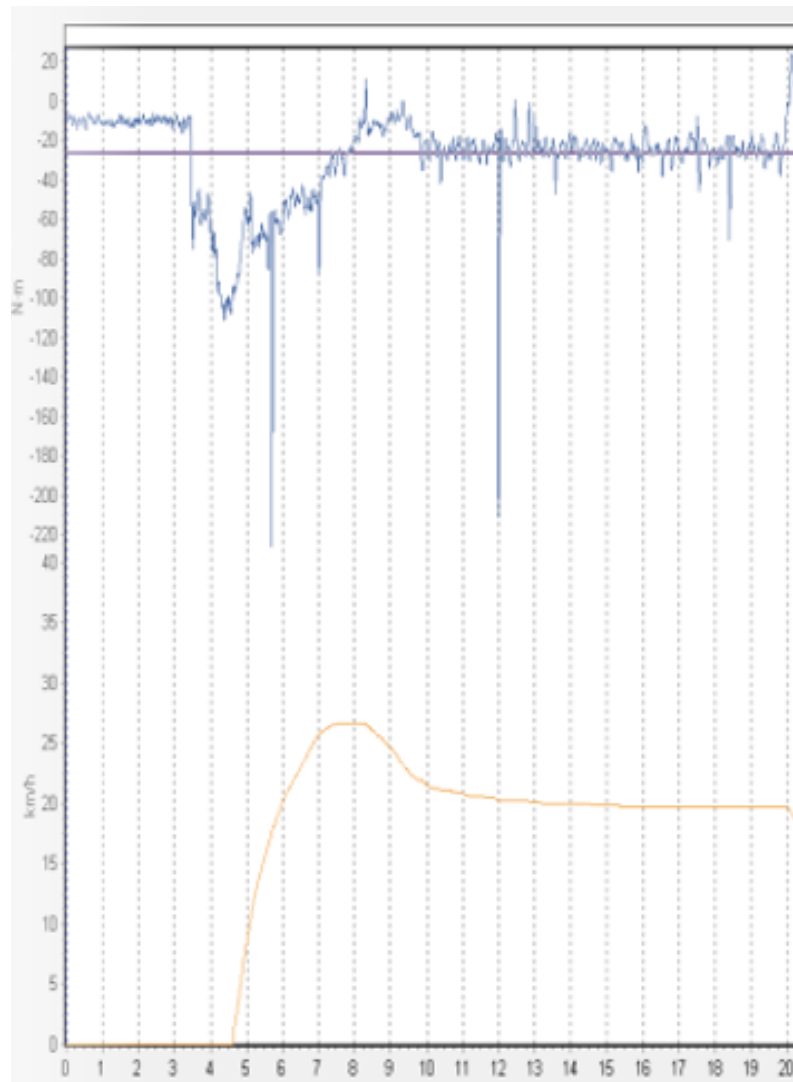


Figure 44. Old measurement data.

The measured velocity (km/h) is presented with yellow as the function of time (s). The measured torque (Nm) is presented with blue as a function of time (s).

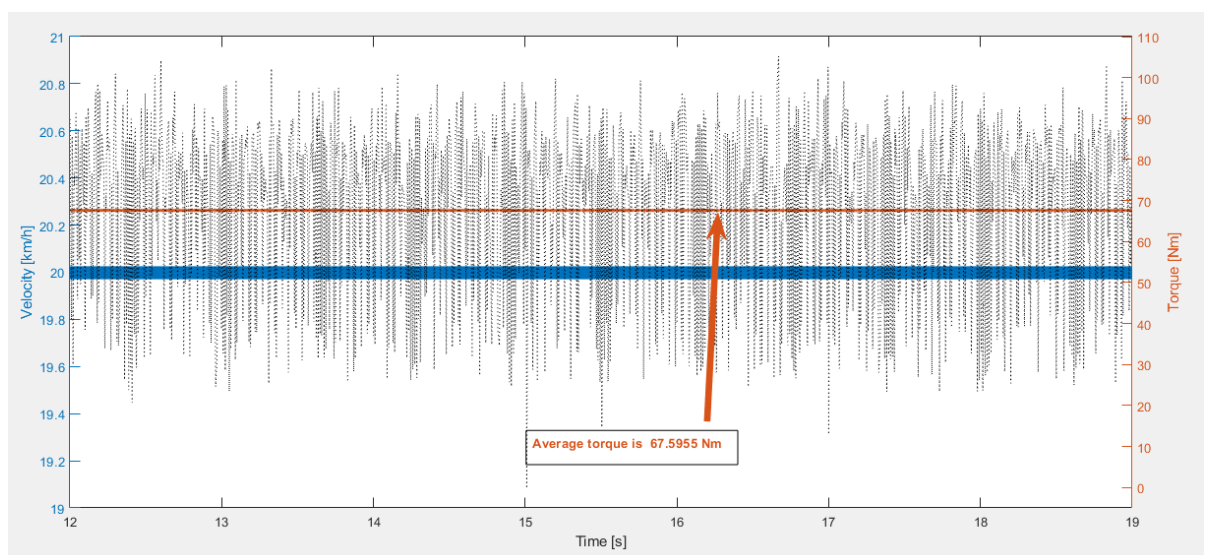


Figure 45. Type 2 20 km/h simulation data.

7.5 Evaluation of the results

The simulated and measured results are evaluated according to the 7.1–7.4 chapters.

7.5.1 Type 1 10 and 25 km/h evaluation

The measured torque with 10 km/h is 11,8746 Nm and the simulated torque on average is 9,9065 Nm (Figure 42). The measured torque is **19,87 %** higher than the simulated torque. As presented in Figure 42 the simulated torque request with 25 km/h is 12,8221 Nm the measured torque is 12,6730 Nm. The simulated torque is **1,17 %** higher than measured torque.

7.5.2 Type 1 50 km/h evaluation

The simulation with 50 km/h run speed is not possible. During simulation excessive vibrations are present causing excessive torque request and instability until the simulation is unable to continue and the model “explodes”. Plausible fixes to the problem could be increasing acceleration time to allow the track vibrations damp and possibly developing a more complex velocity controller function that allows the track velocity to run within few km/h of the requested velocity. Velocity controlling function could also have a functionality to force the torque request to be smoother so the torque increase–decrease cycle is not as aggressive as it currently is with the simple motor. It is also possible that further improvements to the segment connection modelling could be useful to improve the model behaviour on higher velocities. The improvements could consist of adding non-linear material behaviour to every degree of freedom on a segment connection in the future if ATV–plugin allows it. Further studying of the impact–contact modelling on Adams might be also useful. Decreasing contact damping and softening the contact could decrease model vibrations but in the other hand model realism might suffer.

7.5.3 Type 2 20 km/h evaluation

Type 2 validation has uncertainties to the simulation result as the chassis is not a chassis of a real snowmobile. The gear ratio of the measured snowmobile was 2. T_A is presented to be approximately 27 Nm (Figure 44). Therefore:

$$T_R = 27 \text{ Nm} * 2 * 0,95 = 51,3 \text{ Nm} \quad (23)$$

Torque with 20 km/h simulation is 67,5955 Nm (Figure 45). The torque request is **31,77 %** higher than the measured data. As the measured snowmobile and simulated snowmobile are not the same snowmobiles this seems a logical result. Lack of friction measurement data adds uncertainty because with type 2 simulation the track is sliding along track rail all the time unlike with type 1 simulation where the track wobbles all the time and friction contact is not as frequently happening along the track rail–track interface. Further simulations with proper frictions are needed in the future to validate the full vehicle model.

8 CONCLUSIONS

The rear suspension entity model is validated with 10–25 km/h velocities. Model was proved to be accurate with 25 km/h drive speed. 50 km/h simulation was not stable, and 10 km/h simulation demanded less torque than the measured snowmobile. It is likely that model speed limit is between the 25 and 50 km/h, so further simulations are needed as work with the model improvements continue. The 20 km/h full vehicle model was not validated but the model was proven to work as a concept. Full vehicle model validation requests more measured data, especially frictions and work with the chassis model. It should also be noted that with the type of data analysis done the results data is different depending on the simulation time interval used, affecting the resulting average torque

Targets of the study are reached with the rear suspension entity. The model may be used to evaluate the effects of rail bending, track tension, track wheel size, sprocket size, rear wheel size, different sprockets and different track rail materials to the track motion resistances. Contact force study could produce knowledge on how to reduce noises developed by a snowmobile rear suspension entity. Short, high impact forces may cause noises annoying for a human to hear. With the model it could be possible to study how to make contact forces smaller and have longer impact times.

It is recommended to do further validation simulation after all the friction data is available. Building a chassis for the snowmobile will allow simulations as a full vehicle model. Improving the motor model will allow simulating acceleration situations. Bevameter soil tests (on snow) for soft soil are recommended after the full vehicle model is built and validated to simulate and validate the model with soft soil. Adding complex road surfaces i.e., ditches and slopes for simulations could allow simulations of the suspension behaviour in the future.

9 SUMMARY

A snowmobile rear-track suspension entity was built. The built model may be used as a template for evaluating snowmobiles track motion resistances. Different sprockets, wheel sizes, material pairs and tracks may be implemented into the model for simulations to approximate their effect on the track internal motion resistances.

A simulation model of a snowmobile is presented and validated. A rubber track model was implemented instead of a steel track model. Further model improvements are proposed and model usage for different analyses discussed. Theory behind Adams ATV and MBD analyses is discussed, and former knowledge of the tracked vehicle theory is discussed.

The torque demand for the snowmobile track was defined to be within 1,17 % of the measured data while driving 25 km/h. Plausible errors with the model may be incorrect frictions as there was no data measured in time for this thesis. Other plausible error cause is that the track vibrations are too low on higher frequencies as the contacts between track segments and rear suspension parts were empirically softened to a state where the Adams solver was able to integrate time steps forward. Third cause might be that some track segment connection stiffness and dampening values are incorrect as the values that have no measured data are enlightened guesses. Lacking non-linearity on other than the longitudinal x-axis track segment connection is also a possible cause of error. If in the future ATV has a more complex track segment connection model, that allows non-linearity to be added, it should be used to have more accurate behaviour of the track.

The model validation proves that there is still work to do for the model to be accurate especially with higher drive speeds. As is, the model is suitable for studying the effect of changing amount of the track wheels, track wheel sizes, different sprockets, frictions and tracks with speeds under 25 km/h. Higher velocities need more studying and further validation. The model may also be used for evaluating contact forces and therefore, noise sources.

Further model improvements are needed with the measured friction values of the material pairs discussed implemented. For simulations with soft soil, the model could be improved with bevameter snow measurements. Further improvements to the IMPACT and

CONTACT models could be studied for optimizing solving time and making the contacts between objects more realistic as current contacts are implemented to allow maximum stability for simulations.

REFERENCES

Altair, 2022. Using Altair EDEM for Off-road Vehicle Design. [web brochure]
<https://www.altair.com/using-altair-edem-for-off-road-vehicle-design>

Allen P, 2006, Models for Dynamic Simulation of Tank Track Components. [PhD thesis]
 Cranfield University

Campanelli M, Shabana A.A and Choi J.H, 1997. Chain Vibration and Dynamic Stress in Three-Dimensional Multibody Tracked Vehicle. [publication] Multibody System Dynamics 2: p. 277–316, 1998. Available: <https://doi.org/10.1023/A:1009758701296> [referenced 30.5.2022]

Chołodowski J and Dudziński P, 2019. A method for experimental identification of bending resistance of reinforced rubber belts. [publication] AIP Conference Proceedings 2078, 020039 (2019). Available: <https://doi.org/10.1063/1.5092042> [referenced 30.5.2022]

Chołodowski J, Dudziński P.A, Ketting M, 2021. On the energy losses due to tracks vibrations in track crawler vehicles. [article] Archives of Civil and Mechanical Engineering (2021) Available: <https://doi.org/10.1007/s43452-021-00212-8> [referenced 30.5.2022]

Elishakoff I, 2019. Who developed the so-called Timoshenko beam theory? [article] Mathematics and Mechanics of Solids, 25(1), 97–116. Available: <https://doi.org/10.1177/1081286519856931> [referenced 14.6.2022]

Flores P, 2015. Concepts and Formulations for Spatial Multibody Dynamics [book] Springer Cham. ISSN 2191-5318. Available: <https://doi.org/10.1007/978-3-319-16190-7> [referenced 10.6.2022]

Functionbay, 2022. Recurdyn overview [brochure]. Available: <https://support.functionbay.com/en/page/single/2/recurdyn-overview> [viitattu 7.1.2022]

Freedyn, 2022. What is Freedyn [website]. Available: <http://www.freedyn.at/> [referenced 24.11.2022]

McConville J.B, 2015. Introduction to mechanical system simulation using Adams [book] SDC Publications ISBN-13: 978-1585039883

MBDyn org, 2022. Homepage [website]. Available: <https://www.mbdyn.org/> [referenced 7.1.2022]

MSC software, 2022a. Adams Car [brochure]. Available: <https://www.mssoftware.com/product/adams-car> [viitattu 7.1.2022]

MSC software, 2022b. ATV solution [brochure]. Available: https://www.mssoftware.com/Submitted-Content/Resources/TK_Services-ATV_LTR_w.pdf [referenced 24.11.2022]

MSC software, 2021c. Adams help manual, version 2021.2 [user manual]. [referenced 30.5.2022]

MSC software, 2020d. ATV toolkit documentation, soft soil, version 2021.2 [user manual]

MSC software, 2015e, ADM7N2 course notes [user manual]

Makkonen P, 2022. Track parameter definitions [research report]. Metropolia University of Applied Sciences. Available: not available for public use. [referenced 30.5.2022].

Mocera F, Somà A and Nicolini A, 2020. Grouser Effect in Tracked Vehicle Multibody Dynamics with Deformable Terrain Contact Model. [article]. Applied Sciences. 2020; 10(18):6581. Available: <https://doi.org/10.3390/app10186581> [referenced 30.5.2022]

Mocera F and Nicolini A, 2017. Multibody simulation of a small size farming tracked vehicle [publication]. Procedia Structural Integrity vol 8, 2018, p.118–125. Available: <https://doi.org/10.1016/j.prostr.2017.12.013> [referenced 30.5.2022]

Slättenger J. Utilization of Adams to predict tracked vehicle performance. SAE Transactions, 2000, Vol. 109, Section 2: Journal of commercial vehicles pp. 1–7. Available: <https://www.jstor.org/stable/44650730>

Wong J.Y, 2008. Theory of ground vehicles (4th edit.). [book] SBN: 978-0-470-17038-0

A snowmobile with 200 kg of weight carried by the track is running on flat snow surface									
Snow parameters are defined with Wongs presented data (Wong p.130) and enlightened approximations									
n		1,44							
Kc [kN/m ⁿ⁺¹]		10,55							
kφ [kN/m ⁿ⁺²]		66,08							
C [kPa]		6							
φ [deg]		20,7							
c		0,001 (for dynamic simulations)							
Vz [m/s]		0,001							
K [mm]		3							
Snowmobile track is 40 cm wide and 2 meters long with 3 cm grouser height. The grousers are 2 cm wide. Drive sprocket has 90 mm radius									
Snowmobile is driven 40 km/h speed according to the speed sensor but gps shows 39,5 km/h speed									
What is the tractive effort of the snowmobile?									
A general method	Placement	Result	Unit						
Eq. 1 is utilized ->									
p0	9,81 m/s ² * 200 kg / (0,4 m * 2 m) + 0,001 * 0,01 m/s	2452,5 Pa							
Eq.2 is utilized ->									
z	[2452,5 Pa / (10550 N/m ² ,44 / 0,4 m + 66080 N/m ³ ,44)] ^(1/1,44)	0,080414 m							
Eq.3 is utilized ->									
i	(0,5 km/h /3.6 m/s) / (0.092 m * 40 km/h/3,6 m/s/0.092 m)	1,25 %							
Eq 4 is utilized ->									
j	2 m - (1 - 0,0125) * 2 m	0,025 m							
Eq 5 is utilized ->									
tmax	6 000 Pa+ 2452,5 Pa* tan20,7	6926,72 Pa							
Eq 6 is utilized ->									
t	6926,72 Pa * (1 - e ^(-0,0125 m / 0,003 m))	6819,33 Pa							
Eq 7 is utilized ->									
Rt	0,4 m * 1962 * 2 m	1962 N							
Eq 9 is utilized ->									
F	0,4 m * 6819,33 Pa * 2 m	2727,73 N							

Attachment 2 (1/19)

Model definitions on Adams

The sprocket:

Ad Modify a Track Wheel ×

Track Wheel Name

Mass Properties | Geometry (User Entered) | Contact |

Mass

☒ Off-Diagonal Terms

CM Location Relative to Part

Rotation Angle

☒ Fix Rotation Angle

Radial Contact

☐ Ground Contact

Ad Modify a Track Wheel ×

Track Wheel Name

Mass Properties | Geometry (User Entered) | Contact |

Wheel Radius

Wheel Width

Number of Discs Disc Distance

Number of Teeth

Tooth Width Tooth Height

Tooth Length Flank Angle

Rotation Angle

☒ Fix Rotation Angle

Radial Contact

☐ Ground Contact

Attachment 2 (2/19)

Ad

Modify a Track Wheel

×

Track Wheel Name

.hhttest.sprocket.ues_sprocket

Mass Properties

Geometry (User Entered)

Contact

Normal Force

Stiffness

150.0

Damping

1.5

Force Exponent

2.5

Penetration

1.0E-02

Validated Length Unit for Stiffness Coefficient

Millimeter

Friction Force

Static Coefficient

0.6

Dynamic Coefficient

0.5

Stiction Transition Velocity

100.0

Friction Transition Velocity

1000.0

Rotation Angle

128.0

Set

☒ Fix Rotation Angle

Radial Contact

Track Segment Surface

☐ Ground Contact

Track segment:

Ad

Modify Track Segment : Double Segment Rubber Track

×

Track Segment Name

.hhttest.track_geo_v3.ues_trw_segment

Track Pitch

36.8385

Connector Length

36.8385

Pin Radius

2.85

Number of Track Segments

48

Mass Properties

Geometry

Segment Connection

Segment Part

Connector Part

Mass

0.2326168637

lxx

4789.7431950

lxy

-0.406289104

lzx

9.330238E-04

lyy

4783.6861765

lyz

5.52801E-04

lzz

38.885692153

CM Location Relative to Part

-0.7953422354, 6.7374300914, 9.04

Attachment 2 (3/19)

Ad Modify Track Segment : Double Segment Rubber Track ✕

Track Segment Name	.hhttest.track_geo_v3.ues_trw_segment		
Track Pitch	36.8385		
Connector Length	36.8385		
Pin Radius	2.85		
Number of Track Segments	48		

Mass Properties	Geometry	Segment Connection
Segment Part	Connector Part	
Mass	7.96335092E-	
Ixx	1527.832754E	<input checked="" type="checkbox"/> Off-Diagonal Terms
Ixy	-2.18578E-05	Iyy 1538.6998497
Ixz	0.0	Iyz 0.0 Izz 11.286421412
CM Location Relative to Part	0.0, -5.0E-02, 0.0	

Mass Properties	Geometry	Segment Connection
Segment Part (User Entered)	Connector Part (User Entered)	
Plates	Guide	Grouser
Thickness, Inner	2.85	
Thickness, Outer	2.85	
Length, Inner	36.8385	
Length, Outer	36.8385	
Width, Inner	500.0	
Width, Outer	500.0	

Segment Part (User Entered)	Connector Part (User Entered)
Plates	Guide
Number of Guides	2
Guide Type	1
Guide Width	15.0
Guide Height	20.0
Guide Length	25.0
Guide Position	0.0
Guide Distance	304.0

Attachment 2 (4/19)


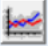
Mass Properties	Geometry	Segment Connection
Segment Part (User Entered)		Connector Part (User Entered)
Plates	Guide	Grouser
Number of Grousers		
1		
1 2 3		
Grouser Position	18.16	0.0
Grouser Angular Position	0.0	
Grouser Height	20.0	
Grouser Width	500.0	
Grouser Length	10.896	

Mass Properties	Geometry	Segment Connection
Segment Part (User Entered)		Connector Part (User Entered)
Plates	Guide	Grouser
Number of Tooth Discs		
2		
Tooth Width	22.877	

Segment Part (User Entered)		Connector Part (User Entered)
Geometry	Guide	
Connector Thickness		
2.85		
Connector Width		
500.0		
Connector Offset		
0.0		

Segment Part (User Entered)		Connector Part (User Entered)
Geometry	Guide	
Number of Conn. Guides		
0		

Attachment 2 (5/19)

Mass Properties	Geometry	Segment Connection
Field Stiffness		
<input type="radio"/> Standard <input type="radio"/> Linear <input checked="" type="radio"/> Nonlinear		
Unload Angle	0.0	
Translational Stiffness	3354.9,1000.0,2000.0	
Translational Damping	2.6696E-02,1.0E-02,2.0E-02	
Rotational Stiffness	2166.4,4660.1,2166.4	
Rotational Damping	2.88E-02,3.9104E-02,2.88E-02	
Crossterm Stiffness	0.0,0.0	
Crossterm Damping	0.0,0.0	
K11 K22 K33 K44 K55 K66		
Nonlinear Stiffness Values	3409.0,550.9,-805.8,213.4	
Frequency Scale Enabled <input type="radio"/> Yes <input checked="" type="radio"/> No		
Field Formulation <input checked="" type="radio"/> Linear <input type="radio"/> Nonlinear		
Field Attachment Offset <input checked="" type="radio"/> Yes <input type="radio"/> No		
Segment Field Attach. Offset	18.41925	
Connector Field Attach. Offset	0	

Attachment 2 (6/19)

Nonlinear Stiffness Parameters	
K_a	3354.9
K_b	3409.0
K_c	550.9
K_d	-805.8
K_e	213.4

X-range	0.0	to	2.0
---------	-----	----	-----

<-- Curve from Parameters

Track rail

Ad Modify a Track Rail ×

Track Rail Name .hhttest.rear_susp_no_wheels.ues_rails

Mass Properties | Geometry (User Entered) | Contact

Mass	9.015674428	
Ixx	1.246697875	<input checked="" type="checkbox"/> Off-Diagonal Terms
Ixy	-4.14538965	Iyy 1.344735075
Izx	5.573335252	Iyz -1.65822428 Izz 1.252792564

CM Location Relative to Part 717.120640886, -277.487119491

Attachment 2 (7/19)

Ad

Modify a Track Rail

×

Track Rail Name

.hhttest.rear_susp_no_wheels.ues_rails

Mass Properties

Geometry (User Entered)

Contact

Major Radius

1020.0

Major Radius Angle Extent

20.0

Major Radius X-position

527.419

Major Radius Y-position

694.341

Minor Radius

20.0

Minor Radius Angle Extent

35.0

Minor Radius X-position

1250.474

Minor Radius Y-position

-323.859

Track Rail Width

10.0

Ad

Modify a Track Rail

×

Track Rail Name

.hhttest.rear_susp_no_wheels.ues_rails

Mass Properties

Geometry (User Entered)

Contact

Normal Force

Stiffness

150.0

Damping

1.5

Force Exponent

2.5

Penetration

1.0E-02

Validated Length Unit for Stiffness Coefficient

Millimeter

Friction Force

Static Coefficient

0.21

Dynamic Coefficient

0.2

Stiction Transition Velocity

100.0

Friction Transition Velocity

1000.0

Attachment 2 (8/19)

Front wheel

Ad Modify a Track Wheel X

Track Wheel Name .hhtttest.rear_susp_no_wheels.uel_f_who

Mass Properties

Geometry

Contact

Mass 0.1604838762

lxx 102.74258654

☐ Off-Diagonal Terms

lyy 102.74258654

lzz 199.467027737

CM Location Relative to Part 0.0, 0.0, 0.0

Ad Modify a Track Wheel X

Track Wheel Name .hhtttest.rear_susp_no_wheels.uel_f_who

Mass Properties

Geometry

Contact

Wheel Radius 52.0

Wheel Width 5.0

Number of Discs 1

Number of Teeth 0

Ad Modify a Track Wheel X

Track Wheel Name .hhtttest.rear_susp_no_wheels.uel_f_who

Mass Properties

Geometry

Contact

Normal Force

Stiffness 150.0

Damping 1.5

Force Exponent 2.5

Penetration 1.0E-02

Validated Length Unit for Stiffness Coefficient Millimeter

Friction Force

Static Coefficient 0.8

Dynamic Coefficient 0.7

Stiction Transition Velocity 100.0

Friction Transition Velocity 1000.0

Attachment 2 (9/19)


Rear wheel

Ad Modify a Track Wheel ×

Track Wheel Name

Mass Properties | Geometry | Contact |

Mass

lxx  ☐ Off-Diagonal Terms

lyy

lzz

CM Location Relative to Part

Ad Modify a Track Wheel ×

Track Wheel Name

Mass Properties | Geometry | Contact |

Wheel Radius

Wheel Width

Number of Discs

Number of Teeth

Ad Modify a Track Wheel ×

Track Wheel Name

Mass Properties | Geometry | Contact |

Normal Force

Stiffness Damping

Force Exponent Penetration

Validated Length Unit for Stiffness Coefficient

Friction Force

Static Coefficient

Dynamic Coefficient

Stiction Transition Velocity

Friction Transition Velocity


Attachment 2 (10/19)

Armwheel

Track Wheel Name: .hittest.rear_susp_no_wheels.uel_r_arm

Mass Properties | Geometry | Contact

Mass: 0.441016884

lxx: 787.75713278  ☒ Off-Diagonal Terms

lxx: 787.75713278

lzz: 1560.09651457

CM Location Relative to Part: 0.0, 0.0, 0.0

Ad

Modify a Track Wheel

✕

Track Wheel Name

.hhttest.rear_susp_no_wheels.uel_r_arm

Mass Properties

Geometry

Contact

Wheel Radius

84.113

Wheel Width

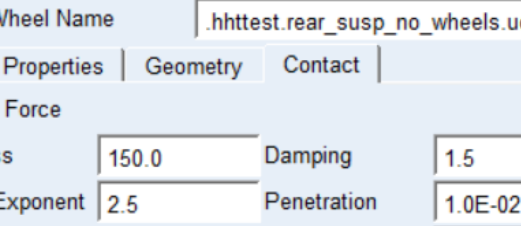
14.483

Number of Discs

1

Number of Teeth

0



The screenshot shows the 'Modify a Track Wheel' dialog box. The 'Track Wheel Name' is '.hhttest.rear_susp_no_wheels.uel_r_arm'. The 'Normal Force' section includes 'Stiffness' (150.0), 'Damping' (1.5), 'Force Exponent' (2.5), and 'Penetration' (1.0E-02). The 'Validated Length Unit for Stiffness Coefficient' is set to 'Millimeter'. The 'Friction Force' section includes 'Static Coefficient' (0.8), 'Dynamic Coefficient' (0.7), 'Stiction Transition Velocity' (100.0), and 'Friction Transition Velocity' (1000.0).

Track Wheel Name	
.hhttest.rear_susp_no_wheels.uel_r_arm	
Normal Force	
Stiffness	150.0
Damping	1.5
Force Exponent	2.5
Penetration	1.0E-02
Validated Length Unit for Stiffness Coefficient	
Millimeter	
Friction Force	
Static Coefficient	0.8
Dynamic Coefficient	0.7
Stiction Transition Velocity	100.0
Friction Transition Velocity	1000.0

Attachment 2 (11/19)

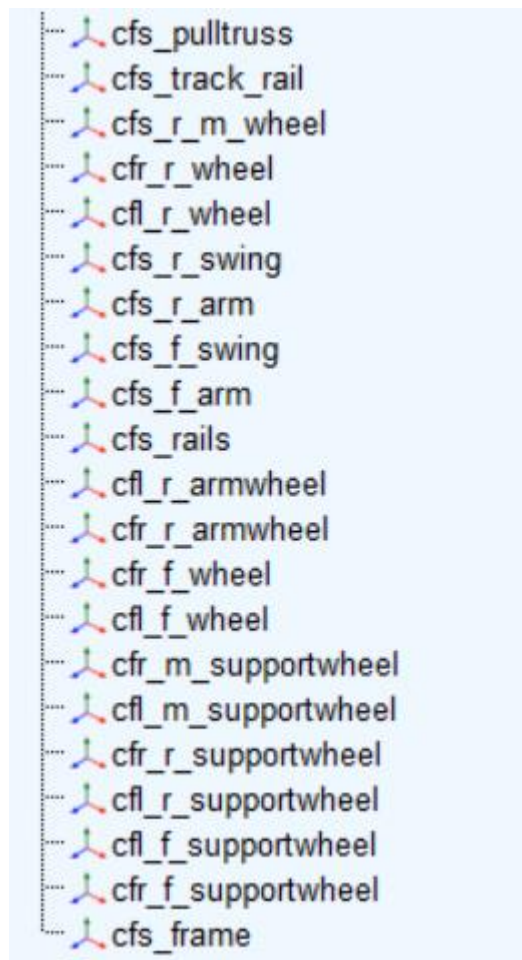
Hardpoints of the rear suspension

	loc_x	loc_y	loc_z
hpl_f_arm_to_frame	262.13	-204.75	-13.115
hpl_f_armaxle	553.982	-112.0	-172.575
hpl_f_supportwheel	433.185	-166.0005	-253.514
hpl_f_swing_lo	621.921	-37.002	-255.325
hpl_f_swing_u	553.982	-52.902	-172.575
hpl_f_wheel	122.652	-61.25	-185.133
hpl_m_supportwheel	600.642	-166.0005	-259.579
hpl_pulltruss_l	623.801	-59.3	-266.165
hpl_pulltruss_u	991.471	-57.302	-95.142
hpl_r_arm_to_frame	1020.123	-225.201	-31.001
hpl_r_armwheel	1020.123	-163.3465	-31.001
hpl_r_supportwheel	1264.119	-166.0005	-264.839
hpl_r_swing_l	1239.917	-112.0	-298.74
hpl_r_swing_u	1263.117	-112.0	-175.645
hpl_r_wheel	1431.048	-165.999	-211.31
hpl_tensioner	1388.629	-165.999	-211.31
hps_f_arm_cm	340.709	0.0	-51.552
hps_f_arm_x	353.15	0.0	-64.5867
hps_f_arm_z	343.15	0.0	-64.5867
hps_f_damper_l	468.781	0.0	-285.276
hps_f_damper_u	284.151	0.0	12.07
hps_f_ropel	122.652	0.0	-185.133
hps_f_rope_u	236.236	0.0	-17.96
hps_f_swing_cm	609.103	0.0	-243.232
hps_f_swing_z	615.248	0.0	-234.575
hps_global_0	0.0	0.0	0.0
hps_pulltruss_cm	895.555	0.0	-135.542
hps_r_arm_bumpstop	1260.724	0.0	-224.87

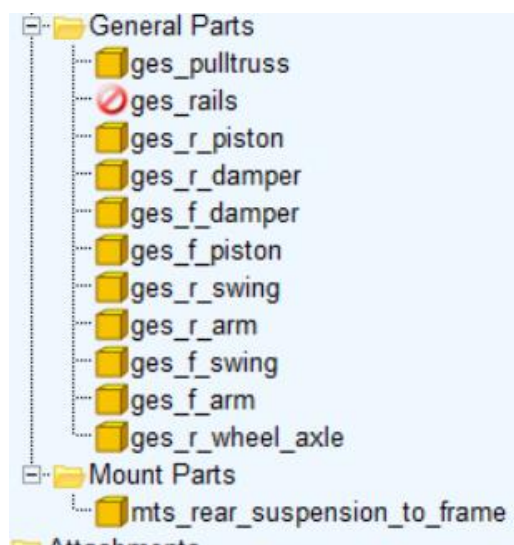
hps_r_arm_cm	1078.726	0.0	-65.794
hps_r_axle_cm	1431.048	0.0	-211.31
hps_r_damper_l	621.921	0.0	-255.325
hps_r_damper_u	1020.809	0.0	11.674
hps_r_m_wheel	1431.048	-64.5	-211.31
hps_r_swing_bumpstop	1260.724	0.0	-224.87
hps_r_swing_cm	1253.514	0.0	-226.488
hps_r_swing_to_arm_CONDITIONAL	1263.117	0.0	-175.645
hps_r_tensioner	1388.629	0.0	-211.31
hps_rails	691.583	0.0	-266.605

Attachment 2 (12/19)

Construction frames



Parts



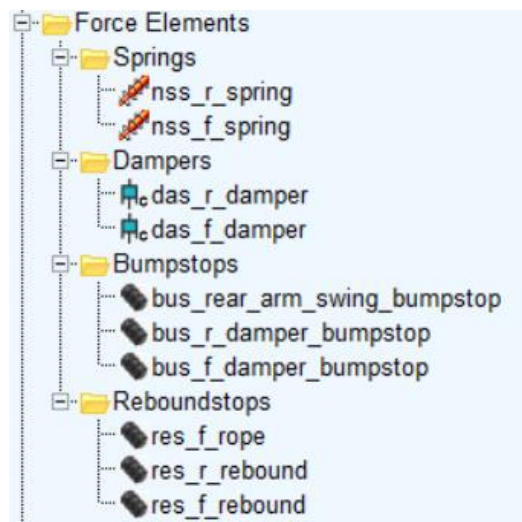
Attachment 2 (13/19)

Joints

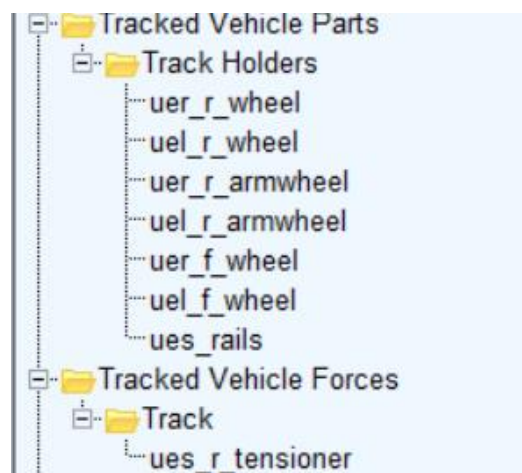
	josinl_pulltruss_u
	josinl_f_arm_to_rails_r
	josinl_f_arm_to_swing
	josinl_r_piston_to_arm
	josinl_f_piston_to_arm
	josinl_r_swing_to_rails_r
	josinl_f_arm_to_frame_r
	josinl_r_swing_to_arm_r
	josinl_r_arm_to_frame
	josrev_pulltruss_l
	jorrev_armwheel
	jolrev_armwheel
	josrev_r_damper_l
	josrev_f_damper_l
	jostra_r_damper
	jostra_f_damper
	jorrev_r_wheel
	jolrev_r_wheel
	jorrev_f_wheel
	jolrev_f_wheel
	jossph_r_swin_to_rails_l
	jossph_r_swing_to_arm_l
	jossph_f_arm_to_swing_l
	jossph_f_arm_to_rails
	jossph_f_arm_to_frame
	jossph_r_arm_to_frame_l
	josfix_rails_mass_rails
	jortra_r_wheel_axle_tension
	joltra_r_wheel_axle_tension
	jostra_r_tensioner

Attachment 2 (14/19)

Forces



ATV parts and forces



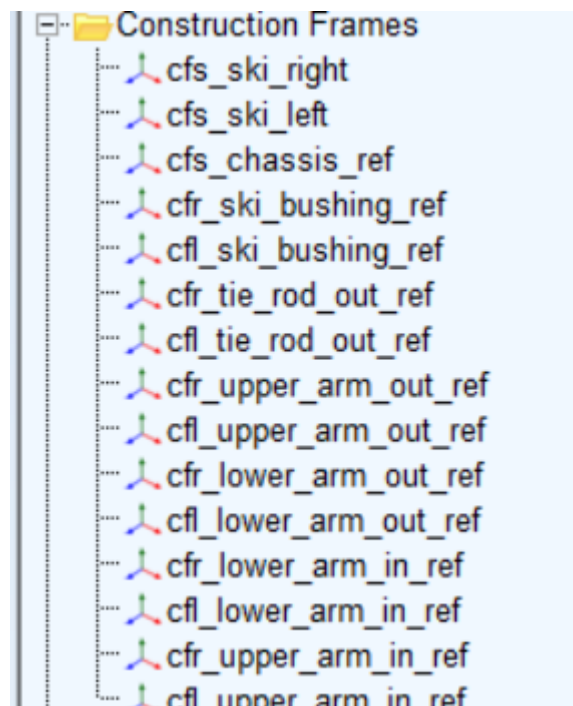
Attachment 2 (15/19)

Front suspension

Hardpoints

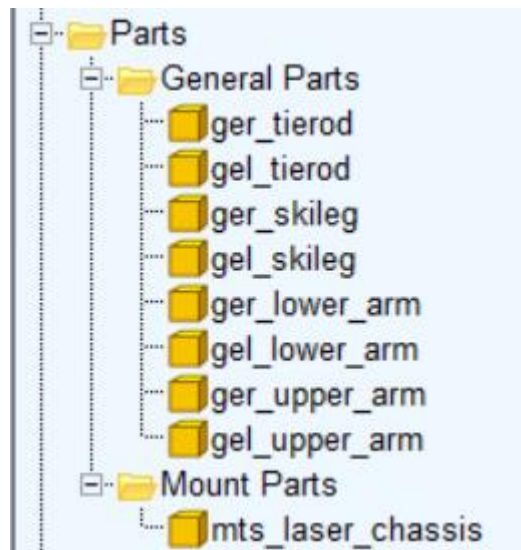
	loc_x	loc_y	loc_z
hpl_lower_arm_front_loc	-761.5125	-13.5	10.1225
hpl_lower_arm_out_loc	-719.037	-520.64	-142.809
hpl_lower_arm_rear_loc	-475.303	-14.0	-40.344
hpl_shock_low_loc	-705.297	-473.277	-93.68
hpl_shock_up_loc	-553.627	-197.924	277.002
hpl_ski_bushing_line_loc	-757.2175	-524.234	-263.988
hpl_skileg_low_loc	-757.2173	-524.2342	-263.9882
hpl_skileg_tierod_loc	-611.965	-527.198	-133.886
hpl_tierod_in_loc	-572.97	-61.926	24.189
hpl_upper_arm_front_loc	-702.387	-172.0	149.477
hpl_upper_arm_out_loc	-659.115	-516.894	5.499
hpl_upper_arm_rear_loc	-503.825	-172.0	114.4655
hps_chassis_loc	0.0	0.0	0.0

Construction frames

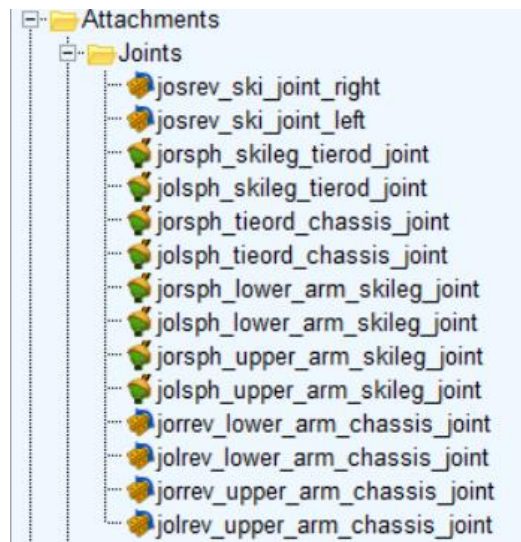


Attachment 2 (16/19)

Parts

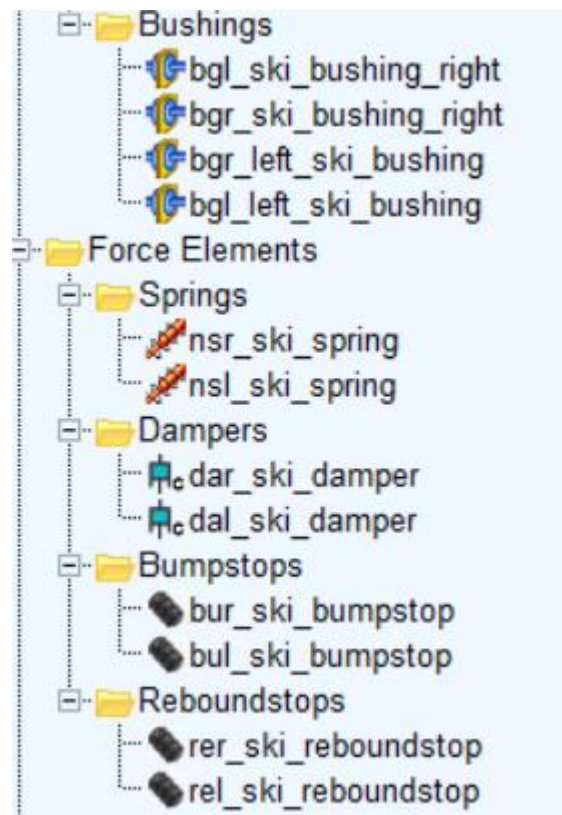


Joints



Attachment 2 (17/19)

Bushings and forces



ATV parts

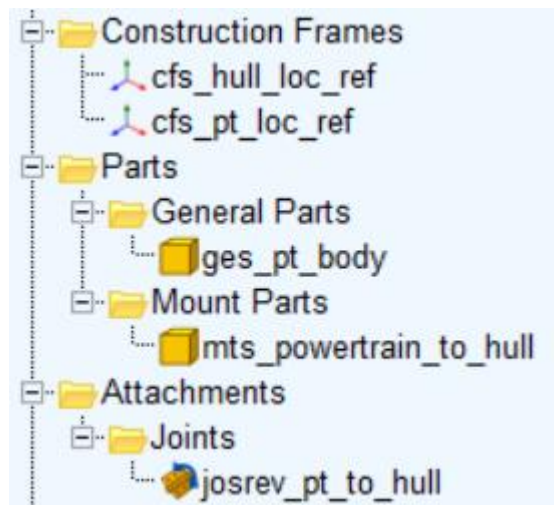
Motor

Hardpoints

	loc_x	loc_y	loc_z
hps_hull_loc	0.0	0.0	0.0
hps_pt_loc	19.501	301.31	-8.948
hps_pt_loc_length	19.501	251.31	-8.948

Attachment 2 (18/19)

Motor parts etc.

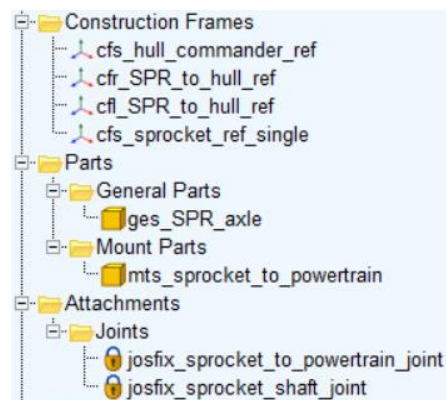


Sprocket

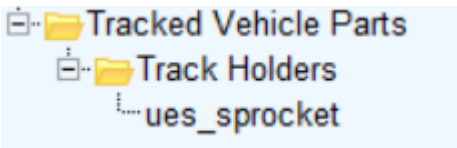
Hardpoints

	loc_x	loc_y	loc_z
hpl_axle_end	19.305	-250.0	-8.658
hps_hull_ref_loc	0.0	0.0	0.0
hps_sprocket_loc_single	19.305	0.0	-8.658
hps_sprockets_joint_loc	25.169	0.0	-17.786

Sprocket parts etc.



Attachment 2 (19/19)

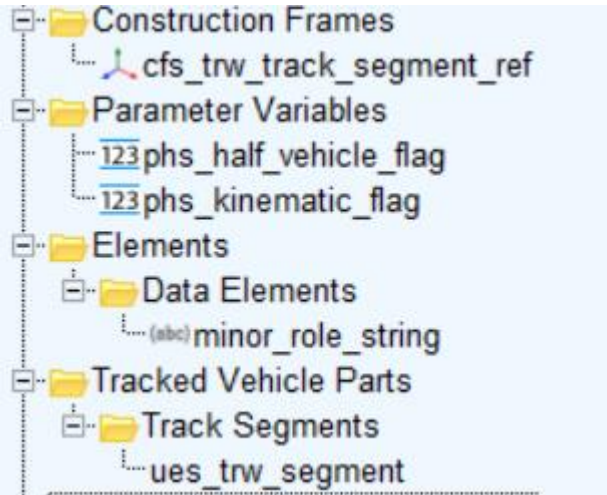


Track segment

Hardpoints

	loc_x	loc_y	loc_z
hps_ref_location	0.0	0.0	0.0

Segment parts etc.



ATTACHMENT 3 1/2

```
%masters thesis model validation
%combined averages of torque as function of speed + original data of ADAMS
%mitatut arvot
m10mv=mean(measured10.v)
m10mt=mean(measured10.t)
m25mv=mean(measured25.v)
m25mt=mean(measured25.t)
nexttile
m10=mean(kmh10.t)
yyaxis right
plot(kmh10.s,m10)
hold on
yyaxis left
plot(kmh10.s,kmh10.v)
yyaxis right
plot(kmh10.s,kmh10.t)
hold off
nexttile
m25=mean(kmh25.t)
yyaxis right
plot(kmh25.s,m25)
hold on
yyaxis left
plot(kmh25.s,kmh25.v)
yyaxis right
plot(kmh25.s,kmh25.t)
hold off
nexttile
m20=mean(asphalt20fr.t)
yyaxis right
plot(asphalt20fr.s,m20)
```


ATTACHMENT 3 2/2

hold on

yyaxis left

plot(asphalt20fr.s,asphalt20fr.v)

yyaxis right

plot(asphalt20fr.s,asphalt20fr.t)

hold off

nexttile

hold on

yyaxis left

plot(measured10.v,m10mt)

yyaxis right

plot(kmh10.v,m10)

hold off

nexttile

hold on

yyaxis left

plot(measured25.v,m25mt)

yyaxis right

plot(kmh25.v,m25)

hold off

nexttile

hold on

yyaxis left

plot(asphalt20fr.v,m20)

yyaxis right

plot(asphalt20fr.v,m20)

hold off